NTNU
Norwegian University of
Science and Technology

Simulation of CO2 Injection in a Reservoir with an Underlying Paleo Residual Oil Zone

Nathaniel Solomon Tadesse

Petroleum Geoscience and Engineering
Submission date: June 2018
Supervisor: Ole Torsæter, IGP
Co-supervisor: Per Arne Slotte, IGP

Norwegian University of Science and Technology
Department of Geoscience and Petroleum

Abstract

Paleo residual oil zones (PROZs) are zones below the oil-water contact (OWC) that contain residual oil. These types of zones exist in many fields around the world, but is often given little attention, due to traditionally being considered unproducible. A modern enhanced oil recovery (EOR) technique that has showed promising results in PROZs is CO_2 injection. Still, companies typically are reluctant to commence CO_2 EOR projects because of the large upfront costs and uncertainty related to how the project will develop. Unforeseen heterogeneities may for example reduce the degree of mixing of CO_2 and oil, even under miscible conditions. It may also lead to unexpected residual oil saturation after injection of CO_2, in parts of the reservoir. Thus, it is important to evaluate effect of CO_2 injection start and CO_2 injection rate. Those parameters influence necessary infrastructure capacity and design. Evaluation of Todd-Longstaff mixing parameter and residual oil saturation to miscible CO_2 injection is also of interest. These are two uncertain parameters that may be dependent on heterogeneities within the reservoir.

In this thesis, sensitivity analysis of CO_2 injection start, CO_2 injection rate, Todd-Longstaff mixing parameter, and residual oil saturation after injection of CO_2 is presented. General trends were noticed; 1. more oil was produced sooner with increased CO_2 injection rate. 2. It seemed beneficial to start CO_2 injection immediately after oil production rate, during waterflooding, had stabilized at a low value. 3. Todd-Longstaff mixing parameter and residual oil saturation after CO_2 injection impacts effectiveness of CO_2 EOR significantly. Substantial amounts of oil was produced from the PROZ and main pay zone (MPZ) in many of the cases ran, when CO_2 was injected, compared to when water was injected throughout. However, most of the extra oil produced came from the MPZ. That will often be the case in field projects as well, and typically it is essential that the MPZ can benefit from CO_2 injection, if CO_2 EOR projects are to be commenced in the PROZ. Furthermore, qualitative comments were provided about economics regarding results of the sensitivity analysis.

Sammendrag

Paleo residuelle oljesoner er soner under olje-vannkontakten som inneholder residuell olje. Disse typer soner finnes i mange felt rundt om i verden, men blir ofte forsømt, fordi de tradisjonelt regnes som ikke-produserbare. En moderne forbedret olje utvinnings-teknikk (EOR-teknikk) som har vist lovende resultater i paleo residuelle oljesoner er CO_2 injeksjon. Likevel er selskpene vanligvis motvillige til å påbegynne CO_2 EOR-prosjekter på grunn av de store forhåndskostnadene og usikkerheten knyttet til hvordan prosjektet vil utvikle seg. Uforutsete heterogeniteter kan for eksempel redusere graden av blanding av CO_2 og olje, selv under blandbare forhold. Det kan også føre til uventet gjenværende oljemetning etter injeksjon av CO_2, i deler av reservoaret. Det er derfor viktig å vurdere effekten av CO_2 injeksjonsstart og CO_2 injeksjonsrate. Disse parametrene påvirker nødvendig infrastrukturkapasitet og design. Evaluering av Todd-Longstaff blandeparameter og gjenværende oljemetning etter blandbar CO_2 injeksjon er også av interesse. Dette er to usikre parametere som kan være avhengige av heterogeniteter i reservoaret.

I denne oppgaven presenteres en sensitivitetsanalyse av CO_2 injeksjonstart, CO_2 injeksjonsrate, Todd-Longstaff blandeparameter og gjenværende oljemetning etter injeksjon av CO_2. Generelle trender ble lagt merke til; 1. mer olje ble produsert raskere med økt CO_2 injeksjonsrate. 2. Det virket gunstig å starte CO_2 injeksjon umiddelbart etter at oljeproduksjonen under vannflømming hadde stabilisert seg på en lav verdi. 3. Todd-Longstaff blandeparameter og gjenværende oljemetning etter CO_2 injeksjon påvirker effektiviteten av CO_2 EOR betydelig. Betydelige mengder olje ble produsert fra paleo residuell oljesone og hovedbetalingssone i mange av scenarioene som ble testet, da CO_2 ble injisert, sammenlignet med når vann ble injisert gjennom hele simuleringen. Imidlertid kom det meste av den ekstra oljen som ble produsert fra hovedbetalingssonen. Det vil også ofte være tilfelle i feltprosjekter, og det er viktig at hovedbetalingssone kan dra nytte av CO_2 injeksjon, hvis CO_2 EOR-prosjekter skal påbegynnes i en paleo residuell oljesone. Videre ble det gitt kvalitative kommentarer om økonomi i forbindelse med resultattolkning av følsomhetsanalysen.

Preface

This master thesis was carried out during the spring of 2018 at the Department of Geoscience and Petroleum, Norwegian University of Science and Technology (NTNU) in Trondheim.

Trondheim, 2018-06-18

Nathaniel Tadesse

Acknowledgment

I would like to thank my supervisor Professor Ole Torsæter (NTNU) and co-supervisor Per Arne Slotte. Their guidance during the course of this project has been essential and their good mood and always open doors has been greatly appreciated.

A special thank you to Per Eirik Bergmo. His inputs have been crucial for the progress om my project.

N.T

Contents

List of Figures

List of Tables

Chapter 1

Introduction

Paleo residual oil zones (PROZs) are zones that exist below the oil-water contact (OWC) and contain residual oil. These zones are a result of the OWC slowly rising a long time before humans interfered with the field. The OWC rise is a result of waterflooding by the nature, over a long time frame. The natural waterflooding may be caused by several mechanisms. Residual oil to the waterflooding will be left between the original OWC and the new, shallower OWC. Traditionally, these zones have been considered unproducible. Hence, little attention has been given to them. However, with modern EOR techniques, significant amounts of the oil in these zones may be produced. Paleo residual oil zones exist below several reservoirs around the world. Due to their spread and effectiveness of modern EOR methods, these zones should be studied in more detail.

Paleo residual oil zones exist in some of the major US basins, like the Willstin Basin, the Permian Basin and the Big Horn Basin (Koperna and Kuuskraa 2006a,b,c). PROZs also exist on the Norwegian Continental Shelf and several other locations in the world. Despite the public literature on EOR projects in PROZs being limited, some results have been reported. Skauge and Surguchev (2000) performed simulations on a reservoir model, to compare CO_2, flue gas and hydrocarbon gas injection in a PROZ. They observed that CO_2 injection was most effective at increasing the oil production. A.A. Aleidan et al. (2014) did laboratory studies on a PROZ core and noticed that it was possible to mobilize the residual oil with CO_2. CO_2 injection in the PROZ has been tested on field scale in the Wasson field (Denver unit), the Seminole Field (San Andres unit), and in the Wasson field (Bennet Ranch unit). Positive results were obtained.

Nonetheless, uncertainties are related to CO_2 EOR projects, because of the related uncertainties and large upfront costs.

The large upfront costs are hard to change. They are reduced if nearby CO_2 infrastructure solutions and proximity to a pure CO_2 stream exists. If that does not exist, vast amounts of money are needed to implement suitable solutions. To avoid spending unnecessary amounts of money, it is important to know when the CO_2 injection should start and at what rate. This is so that solutions with sufficient capacity can be constructed, without paying for more than you need.

The goal of this thesis is to evaluate effect of CO_2 injection rate and CO_2 injection start time on the oil production. Assessing the effect of two uncertain parameters; miscible residual oil saturation and Todd-Longstaff mixing parameter is also an objective. This is because companies often are reluctant to do CO_2 EOR projects beacause of up front costs and uncertainties, therefore it can be of interest to see the significance of uncertain parameters. Another purpose of this thesis is to give a solid basis for understanding the potential of PROZs, a type of zone that often is neglected despite containing substantial amounts of oil.

In chapter 2 and 3, theory about PROZs, CO_2 EOR, and CO_2 injection in PROZs are presented. Similar approach was used to qualitatively inspect the effect of CO_2 injection rate and CO_2 injection start on oil production, in addition to effect of the two uncertain parameters; Todd-Longstaff mixing parameter, and miscible residual oil saturation. The approach was to perform simulations on a synthetic reservoir model. The procedure to construct the synthetic model is described in chapter 4. In chapter 5 results of the sensitivity analysis are presented and in chapter 6, the results are discussed.

Chapter 2

Paleo Residual Oil Zone

The traditionally producible reservoir zone above the owc predominantly contains mobile oil, and is often called the conventionally productive zone or the main pay zone (MPZ). However, in many reservoirs around the world, an additional oil zone exists below the oil-water contact (owc), even before humans have interfered with the reservoir through production and/or injection of fluids. This additional zone is usually referred to as the residual oil zone and is illustrated in **Fig. 2.1**. Zones like this may exist where the reservoir has been waterflooded naturally over a long period of time, meaning that the original OWC was deeper than what currently is observed. The main focus through this thesis will be these types of naturally caused residual oil zones, and to distinguish them from zones flooded under human influence, the term paleo-residual oil zone will be used.

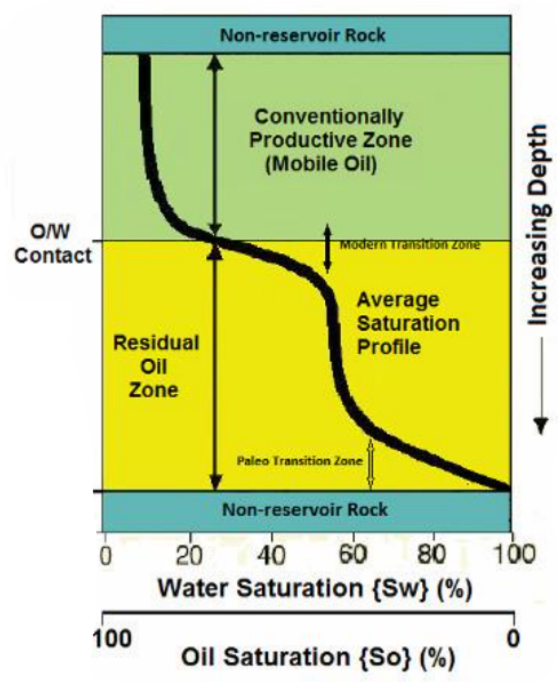

Fig. 2.1—The graph shows a saturation profile, with high oil satiration above the owc i.e in the mpz and a lower oil sat in the residual oil zone below the owc. A transition zone exists between the MPZ and the ROZ (*Curtesy of Research Partnership to Secure Energy for America (RPSEA)*).

2.1 Origin of paleo residual oil zones

Paleo residual oil zones (PROZs) may occur as a result of several natural events. Melzer et al. (2006) discuss three normal causes of PROZs; 1. regional or local basin tilting, 2. altered hydrodynamic flow fields and 3. breached and reformed seals. Each of these three processes can be thought of as natural waterflood after an initial accumulation of oil in the subsurface trap (Melzer et al. 2006).

2.1.1 Regional or Local Basin Tilt

Paleo residual oil zones as a result of basin tilting, arises from a gravity dominated shift of oil and underlaying water in a trap (Melzer et al. 2006). In **Fig. 2.2** a hypothetical hydrocarbon accumulation is depicted and in **Fig. 2.3**, the same entrapment is depicted after it has undergone a westward regional tilt. In Fig. 2.2, a spill point in the entrapment can be spotted in east. After the entrapment has undergone a regional westward basinal tilt, the spill point in east is preserved, causing oil to escape in east, while the entrapment is being waterflooded by an aquifer in the west. Hence, the residual oil zone is thickest in the west and declines eastwards, as shown in Fig. 2.3. These types of residual oil zones may contain a lot of residual oil, if the regional tilt is considerable and/or the field is of substantial size (Melzer et al. 2006). Fig. 2.3 also shows that the base of oil saturation has been tilted, while the OWC of movable oil is controlled by gravity and therefore is horizontal (Trentham et al. 2012).

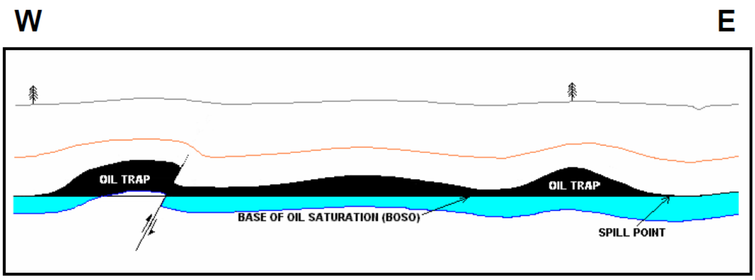

Fig. 2.2—An original hydrocarbon accumulation (a hypothetical example) (*Trentham et al. 2012*).

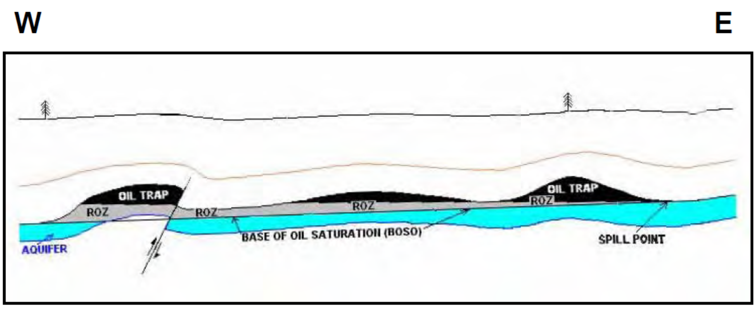

Fig. 2.3—Here the original (hypothetical) entrapment has undergone a westward regional tilt and oil has escaped in east, while the entrapment is being waterflooded by an aquifer in the west. Thus, the residual oil zone is thickest in the west and declines eastwards (*Trentham et al. 2012*).

2.1.2 Breached and Reformed Reservoir Seals

Fig. 2.4 depicts another type of paleo residual oil zone. In the type of PROZs presented in that figure, the initial reservoir seal has breached. Next, part or all of the oil may escape the reservoir, since the reservoir seal has been breached. Then a new seal may be formed, or the old seal gets healed, creating a new entrapment. If the new entrapment contains a thinner oil column than the initial entrapment, a residual oil zone will be present. This procces of breaching and healing a reservoir seal may happen under several circumstances. The seal may for example breach because of buildup of fluid pressures during the formative reservoir stage (Melzer 2006). The resealing on the other hand, may be a result of geochemical or biological processes. To prove that a PROZ was created by breaching and reforming reservoir seals is usually not trivial. However, presence of tar mats and other solid hydrocarbons within the oil column may be an indication of these processes. The base of oil and the OWC will be horizontal in these zones.

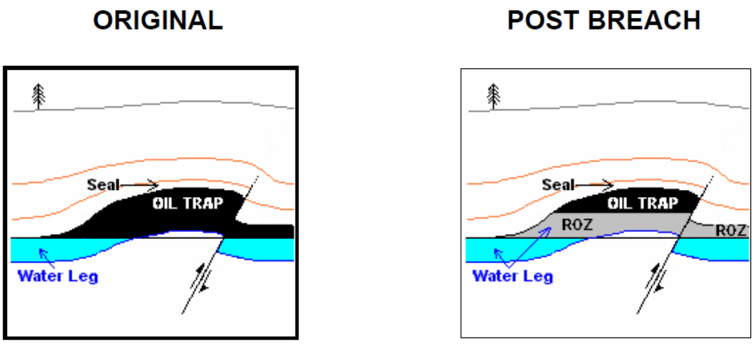

Fig. 2.4—A reservoir seal may be breached and then resealed. Between the breaching and resealing, oil may escape and a PROZ may be formed (*Trentham et al. 2012*).

2.1.3 Altered Hydrodynamic Flow Fields

Changed hydrodynamic conditions within aquifers of an oil basin is a normal cause of paleo residual oil zones. Distant or nearby uplift of the regional formation is often the root of changed conditions (Melzer et al. 2006). The entrapment shown in **Fig. 2.5** had the entrapment shown in Fig. 2.2 as its original entrapment. Yet, changed hydrodynamic conditions lead to a residual oil zone. In Fig. 2.5 a west to east hydrodynamic flow field is used to explain the tilted OWC. The OWC is tilted because of the hydrodynamic forces on the oil column. With adequate information, it is possible to calculate the hydrodynamic flow field responsible for the tilt with Eq. 2.1 (Melzer 2006)

$$\frac{dz}{dx} = -\frac{dp}{dx}\frac{\rho_w}{\rho_w - \rho_o}, \quad \text{...} \quad (2.1)$$

where:

$\frac{dz}{dx}$ = OWC tilt
$\frac{dp}{dx}$ = Pressure (potentiometric) gradient of the aquifer
ρ_w = water density in the aquifer
ρ_o = oil density

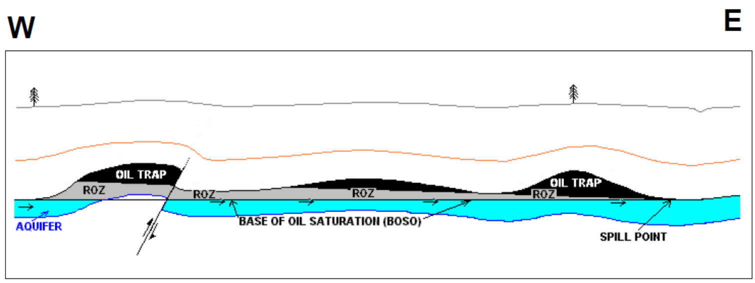

Fig. 2.5—Paleo residual oil zones may be caused by altered hydrodynamic conditions within aquifers of an oil basin. (*Trentham et al. 2012*).

2.2 Paleo Oil

One of the things that make paleo oil zones so interesting is the large amounts of extra oil that potentially can be produced with modern enhanced oil recovery (EOR) methods. To decide which EOR method to use, it is crucial to know the oil properties. Commonly, when a reservoir has been, or is going to be produced, the oil from the main pay zone has been tested extensively. Thus, the oil properties are mostly known. However, properties of the oil in the main pay zone and oil in the PROZ may differ. That could be a result of oil in the PROZ interacting with water over a long period of time. Hence, oil in the PROZ should also be sampled and tested, to decide the proper EOR method. There are not many detailed analysis of paleo oil in the literature, because it can be hard, expensive and unnecessary to obtain a sample. Nonetheless, A. Aleidan et al. (2017) presents a detailed analysis, providing comparisons between paleo oil and oil from the main pay zone.

2.2.1 Studies by A. Aleidan et al. (2017)

The studies executed by A. Aleidan et al. (2017) inspects paleo oil from reservoir sponge cores, which were taken from the PROZ of a producing reservoir, and compares it with oil from the main pay zone. It was noticed that the overall composition and quality of the paleo oil was similar to the MPZ oil. Yet, when doing a more thorough analysis on molecular level, significant differences were observed. These differences could be significant enough to influence the decision of which EOR method to use.

The cores used in the study were in their native state. They used three types of fluids for the laboratory core flooding. The three fluids were; surfactant solution, 0.1 wt %-S887 in seawater, toluene and finally supercritical CO_2 (sc-CO_2). Pyrolic oil productivity index (POPI) can be used to give indications of the oil quality (Jones and Tobey 1999), as it was done for the paleo oil and MPZ oil. The results indicated similar quality of the two oils. Furthermore, to decide the filling history and source rock of the oil samples, A. Aleidan et al. (2017) used gas chromatography coupled with flame ionization detector (GC-FID). It was noted that the pristane/phytane ratio was equal to 0.58 for the paleo oil, while it was 0.63 for the MPZ oil, indicating that they had the same source rock, a Jurassic oil from a carbonate source. **Fig. 2.6** shows the GC-FID signatures for the paleo and MPZ oil. The overall signatures show differences, but the ratios are similar, confirming the same source rock. In addition, bio marker analysis tests were performed to confirm the source rock and similarities between the paleo and MPZ oil. In **Fig. 2.7**, the bio-markers signature of the paleo and MPZ oil are shown, and it can be seen that the pattern of the tricyclic and tetracyclic compounds are very similar. The mentioned pattern is frequently used to determine the source rock depositional environment and organic facies. Therefore, the bio-markers signature supports the theory that the paleo oil and MPZ oil are relatively similar and come from the same source rock.

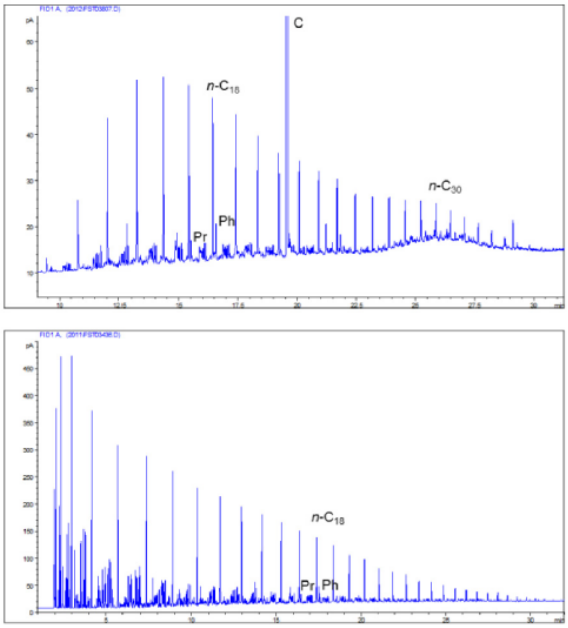

Fig. 2.6—GC-FID signatures. Signature for the paleo oil is shown on the top, while the MPZ oil signature is shown on the bottom (*A. Aleidan et al. 2017*).

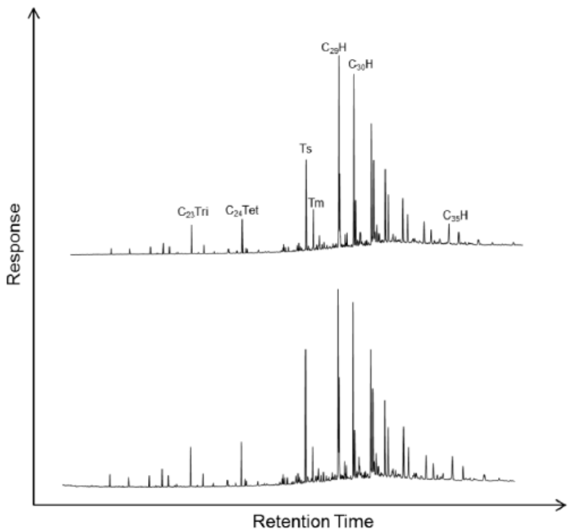

Fig. 2.7—Bio-markers signatures of MPZ on the bottom and of paleo oil on the top (*A. Aleidan et al. 2017*).

A. Aleidan et al. (2017) also analyzed the paleo and MPZ oil using simulated distillation. They observed that the components from C5 to C11 and heavier components from C24 were lacking in the paleo oil. The components from C12 to C23 on the other hand, were abundant. That was not the case for the MPZ oil, where the components from C5 to C11 existed in large amounts and C12 to C23 in smaller amounts. This component distribution is of great importance for the choice of EOR method, meaning that the optimal EOR method for the PROZ cannot necessarily be deduced based on information about the MPZ oil, but rather on information about the paleo oil.

A. Aleidan et al. (2017) also investigated the NMR T2 distributions of paleo oil produced with CO_2 injection from two different reservoirs and compared it to the MPZ oil of the respective reservoirs, as illustrated in **Fig. 2.8**. The figure shows fairly similar paleo and MPZ oil T2 distributions for both reservoirs, but with evident differences. For the reservoir in Fig. 2.6a, it is clear that the paleo oil is missing intermediate hydrocarbon components unlike the MPZ oil. Paleo oil from the reservoir in Fig. 2.6b however, is missing the light hydrocarbon components and has a large portion of heavy components compared to the MPZ oil.

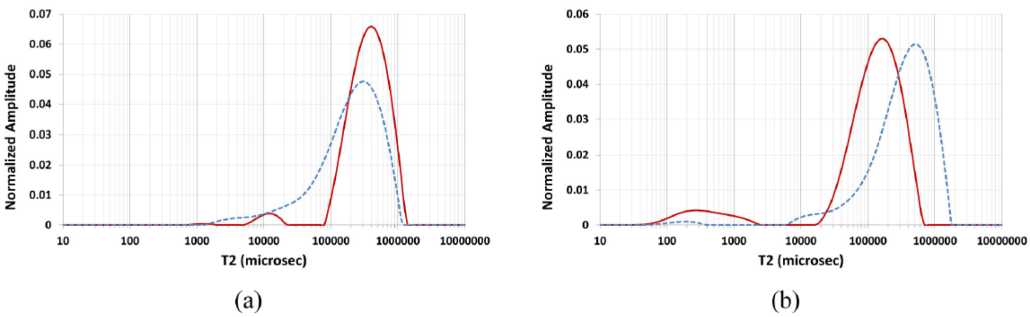

Fig. 2.8—NMR T2 distributions from two different reservoirs. In each reservoir the NMR T2 distributions of paleo oil (red) is compared to MPZ oil (blue) (*A. Aleidan et al. 2017*).

2.3 Spread of Paleo Residual Oil Zones

Production from a paleo residual oil zone (PROZ) is not straightforward and usually demands tertiary recovery techniques. However, the spread of these zones and extent of oil there makes PROZs an important topic. Several reports by the US Department of

Energy (DOE) documents the existence of extensive paleo residual oil zones that may be produced through CO2 injection. The reports estimate the amount of producible oil from PROZs in some of the major US basins; the Willistin Basin, the Permian Basin and the Big Horn Basin (Koperna and Kuuskraa 2006a,b,c). For the basins combined, the estimations presented in reports suggest that the total amount of recoverable paleo residual oil is approximately 8 GSm^3.

Moreover, recovery from PROZs has been studied in two Chinese basins by Liu et al. (2006) and Pang et al. (2012), while Yang (2014) investigated PROZs in southwest Saskatchewan, Canada. Similar studies have been executed on the Norwgian Continental Shelf (NCS), for instance by Skauge and Surguchev (2000), who studied recovery of oil in the PROZ at the Troll field. Furthermore, in a study for Statoil, Bergmo et al. (2018) mapped the existence and extent of oil in PROZs, as well as the potential for CO2-EOR, in several Statoil operated fields on the NCS. More than 40 fields were initially considered, and in 20 of those fields they found evidence of a PROZ. Nevertheless, they state that the information available was very restricted and that it is likely that more of the fields had a PROZ. The fields with evidence of a PROZ were located in the North Sea, the Norwegian Sea and one in the Barents Sea. Bergmo et al. (2018) estimated the PROZ resources of the 20 fields with a simple volumetric approach, using the field area, thickness of the PROZ, oil saturation in the PROZ, porosity, formation volume factor and areal fraction. The fraction of a field that is assumed to have a PROZ is represented by the areal fraction. Due to lack of information, they made some simplifications, leading to conservative estimates. Oil saturation of all PROZs were set to 10 %, and other assumptions were made as well. The areal fraction and net thickness are two highly uncertain parameters in their estimates. Nonetheless, the results of their estimations are presented in **table. 2.1**, which shows that more than 1 GSm^3 of oil might exist in total, in the PROZs of the fields in their study. Some of the fields like Veslefrikk, Troll and Snøhvit are major contributors to this number. Despite uncertainty in some of the parameters, it seems probable that the amount of resources is at least in the order of 1 GSm^3, considering the conservative assumptions. Thus, PROZs and potential EOR methods should be considered mor carefully on the Norwegian Continental Shelf.

Table 2.1—Estimations of parameters and paleo residual oil in place for different fields. (*Bergmo et al. 2018*).

Fields	**Area**	**Thickness**	**Saturation**	**Porosity**	**B_o**	**Eff. Area**	**OIL**
	km^2	**m**	**Fraction**	**%**	**Rm^3/Sm^3**	**Fraction**	**$MMSm^3$**
Alve	12.6	2	0.1	25	1.2	1	**0.5**
Fram	31.8	25	0.1	25	1.2	0.5	**8.3**
Glitne	9.4	2	0.1	25	1.2	1	**0.4**
Grane	40.1	74	0.1	25	1.2	1	**61.9**
Gullfaks	62.0	60	0.1	27	1.4	0.8	**57.4**
Gullfaks-Sør	72.2	70	0.1	17	1.6	0.5	**26.8**
Heidrun	38.9	25	0.1	25	1.2	0.5	**10.1**
Heimdal	37.5	40	0.1	26	1.2	0.5	**16.3**
Huldra	22.0	93	0.1	25	1.20	1	**42.7**
Oseberg	155.2	15	0.1	23	1.43	0.7	**26.2**
Oseberg-Sør	98.6	50	0.1	25	1.2	0.7	**71.9**
Skuld	6.5	25	0.1	25	1.2	0.5	**1.7**
Snorre	108.3	15	0.1	24	1.33	1	**29.3**
Snøhvit	360.2	200	0.1	15	1.44	0.5	**375.3**
Statfjord	91.7	95	0.1	21	1.54	0.3	**35.6**
Tordis	32.1	12	0.1	25	1.2	0.8	**6.4**
Troll	642.7	40	0.1	27	1.18	0.2	**117.7**
Tyrihans	50.1	15	0.1	25	1.2	0.5	**7.8**
Vega	18.2	6	0.1	25	1.2	0.8	**1.8**
Veslefrikk	33.3	200	0.1	25	1.2	1	**138.7**
Total							**1035.1**

Chapter 3

CO_2 Enhanced Oil Recovery

In most oilfields, large energy resources are left behind in the reservoirs, because the production at some point stops being economically favorable or most of the remaining oil is immobile. Some zones stop being economically favorable at oil saturations above 60%, while other zones may be produced until the residual oil saturation (S_{or}) is reached. The oil remaining at residual oil saturation is considered immobile. However, with modern enhanced oil recovery (EOR) techniques, even the residual oil may be produced. CO_2 EOR has been used since the 1970s (Zhang et al. 2010). The CO_2 will under ideal conditions mix with the oil to make it flow more easily. If required volumes of non-expensive CO_2 is available, CO_2 injection has proved to potentially be an effective EOR method.

Several advantages and challenges are related to CO_2 EOR. One obvious advantage is that the injected CO_2 may increase the oil recovery. Also, CO_2 can be cheaper than other similarly miscible fluids. Another important aspect is the environmental aspect, as CO_2 EOR projects give the opportunity to reduce greenhouse gas emissions. CO_2 may for instance be extracted from the exhaust of gas-fired turbines and compressed for injection (McKean et al. 1999). When CO_2 is injected in the reservoir to extract more oil, some of the CO_2 will be left and stored in the reservoir, instead of potentially being emitted to the atmosphere. Influence of human activity on global warming is still being scientifically discussed, but today there is a large consensus that greenhouse gases, among them CO_2, contributes to global warming. Thus, different initiatives have been introduced to make eco-friendly measures more profitable for companies. For instance, companies are given permits to emit a certain amount of CO_2.

Companies that reduce their CO_2 emissions are allowed to sell excess permits to companies that do not meet the emission restrictions. Hence, expenditures are related with CO_2 EOR, but since it also may lead to CO_2 sequestration, the companies CO_2 emission may be reduced which in turn may generate extra income (or less expenditures) due to the current advantages of eco-friendly measures. Therefore, the value created by resulting CO_2 sequestration may cover some of the costs related to CO_2 EOR. The extra amount of oil possible to produce with CO_2 EOR is of course decisive for how economically favorable the process is.

It is possible to combine CO_2 EOR and CO_2 storage. Nevertheless, the focus of CO_2 EOR is to increase the recovery factor of oil, while CO_2 storage focuses on storing as much CO_2 in the reservoir as possible. Hence distinctive designs will be required for optimization, depending on what the ultimate goal is. In this chapter the focus will be on CO_2 EOR, but it should be kept in mind that despite the focus being on increasing the oil recovery, substantial amounts of the injected CO_2 will be left in the reservoir, which may give further financial benefits.

3.1 History of CO_2 EOR

During the 1960s, the possibility of performing tertiary recovery to extract oil from reservoirs after waterflooding, was investigated. Several injectants were tested and CO_2 proved to be an injectant with the potential to increase the oil recovery. In the early 1970s, the first commercial CO_2 EOR injection project was carried out. In the late 1970s, CO_2 EOR proved its viability, since the SACROC and North Cross CO_2 injection projects were showing positive results. In the 1980s, several companies investigated infrastructure necessary to perform CO_2 EOR (Melzer 2006). Following, the CO_2 EOR industry has continued to grow. Several projects indicated that injection of CO_2 could be a successful way of increasing the recovery factor. Even projects where waterflooding had swept the reservoir well, to oil saturations of approximately 30%, has shown that further production can be economically favorable with injection of CO_2, bringing the residual oil saturation down to 15% in some cases. Observations like that made paleo residual oil zones an interesting target for CO_2 EOR.

3.2 Principle Behind CO_2 EOR

During the lifetime of a field, production of oil typically becomes more challenging with time. There can be several reasons for this development. For example, the pressure may drop or the remaining oil may be thick and unable to flow. One solution to the pressure drop could be water injection, which may increase or maintain the reservoir pressure and help push oil to the production well. However, it is restricted how much oil that can be produced by waterflooding, and other EOR methods are often used after the reservoir has been waterflooded, or even before/instead of waterflooding.

CO_2 EOR may be employed on a field and during this process compressed CO_2 is injected into the reservoir. The CO_2 will act like a solvent, making the oil expand and flow more easily towards production wells (PTRC 2014). There are especially two characteristics of CO_2 that makes it a good choice for EOR: it is miscible with oil under conditions that often are fulfilled in a reservoir, and secondly it is cheaper than many other similarly miscible fluids. CO_2 may displace oil by various mechanisms, but to understand these, some CO_2 characteristics should be understood.

3.2.1 CO_2 Characteristics

CO_2 injection can be effective and following are some characteristics of CO_2 injected into a reservoir: "1. It promotes swelling. 2. It reduces oil viscosity. 3. It increases oil density. 4. It is highly soluble in water. 5. It exerts an acidic effect on rock. 6. It can vaporize and extract portions of crude oil. 7. It is transported chromatographically through porous rock" (Holm and Josendal 1974). Swelling is caused by the high solubility of CO_2 in oil. Nonetheless, it should be noted that the solubility is different in gas saturated reservoir oil and stock-tank oil. Stock tank oil is expanded to a larger degree than the reservoir oil. Also, CO_2 swells an oil more than what methane does, but when CO_2 is injected into a reservoir, it does not displace all of the methane, meaning that less of the CO_2 goes into the oil, resulting in less swelling of reservoir oil (Holm and Josendal 1974). Crude oils become significantly less viscous as they get saturated with CO_2, and the more viscous crudes have a larger percentage reduction in viscosity (Beeson and Ortloff 1959; Holm 1963; Simon and Graue 1965). According to Crawford et al. (1963), injectivity of water is increased by the acidic effect of CO_2, due to direct action on carbonate portions of the rock and a stabilizing action on clays in the rock. There are various mechanisms by which CO_2 may displace oil from porous media, and following some of these mechanisms are discussed.

3.2.2 Solution Gas Drive

The first mechanism to be discussed is solution gas drive. CO_2 is a gas and as pressure is increased, an increasing amount of CO_2 may go into solution with oil. When the pressure is decreased again, the CO_2 may go out of the solution again as free gas and create a solution gas drive. An experiment has been performed to illustrate this process (Holm and Josendal 1974). Their experiment was conducted on a 4 ft long Berea sandstone, that was saturated with 47 % heavy, low-gravity stock-tank oil and 53 % brine at 900 psi. CO_2 was then injected at 900 psi, to saturate a portion of the oil. Next, the pressure was reduced to 400 psi and during the pressure reduction, 14.2 % of the oil in place was produced. Then the pressure was reduced to 200 psi and during that process 4.5 % of the remaining oil in place was produced. **Table. 3.1** shows the amount of oil produced, as the pressure was decreased. Solution gas drive with CO_2 was simply the production mechanism for the test. The produced crude oil had approximately the same characteristics as injected crude oil (Holm and Josendal 1974). However, this production technique is not common for CO_2 EOR in commercial fields.

Table 3.1—Oil is recovered as the pressure is decreased, by solution gas dive. A 4 ft long Berea sandstone containing heavy, low-gravity stock-tank oil and brine was used for the experiment. CO_2 was injected at 900 psi, before pressure reduction started. (*Holm and Josendal 1974*).

Pressure (psig)	Oil Recovered (percent of oil in place)	Oil in Place (percent PV)
900	—	47.2
400	14.2	40.5
200	18.6	38.4

3.2.3 Immiscible Contra Miscible CO_2 Drive

An important trait of CO_2 is its ability to vaporize or extract hydrocarbons from an oil. Menzie and Nielsen (1963) demonstrated this. They observed that more than 50 % of a 35° API crude oil was vaporized and extracted at 135°F and 2000 psi. Most extraction of oil takes place only above a certain pressure, this pressure varies depending on temperature of the crude oil, as illustrated in **Fig. 3.1**. Transfer of portions of the oil above a certain pressure to the CO_2 phase causes the oil shrinkage illustrated in Fig. 3.1. The CO_2 to oil ratio is 2.5:1, and decreasing that ratio (but still having enough CO_2 to saturate the oil) would lead to less oil being extracted, but the pressure at which extraction begins would remain the same. In **Fig. 3.2**, the oil recovered by CO_2 floods is plotted vs flooding pressures for a crude oil temperature of 135°F. Both amount of oil produced at CO_2 breakthrough and at end of flood is shown. It can be observed that amount of oil recovered increases drastically with increasing flooding pressure until a certain pressure is reached. Miscible-type displacement with oil recovery above 93 % is achieved with flooding pressure of 1900 psi, and when comparing to Fig. 3.1, it can be seen that a lot of oil has been extracted at this pressure. Further inspection revealed that it was mostly the middle boiling range hydrocarbons that were extracted.

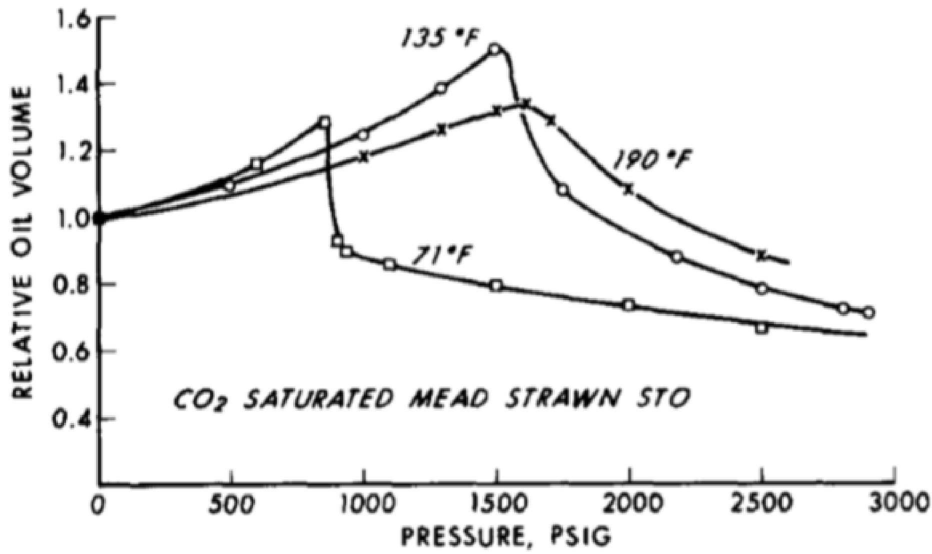

Fig. 3.1—Volume change of stock tank oil as CO_2 is added under increasing pressure. Above a certain pressure, major extraction of hydrocarbons from crude oil happen (*Holm and Josendal 1974*).

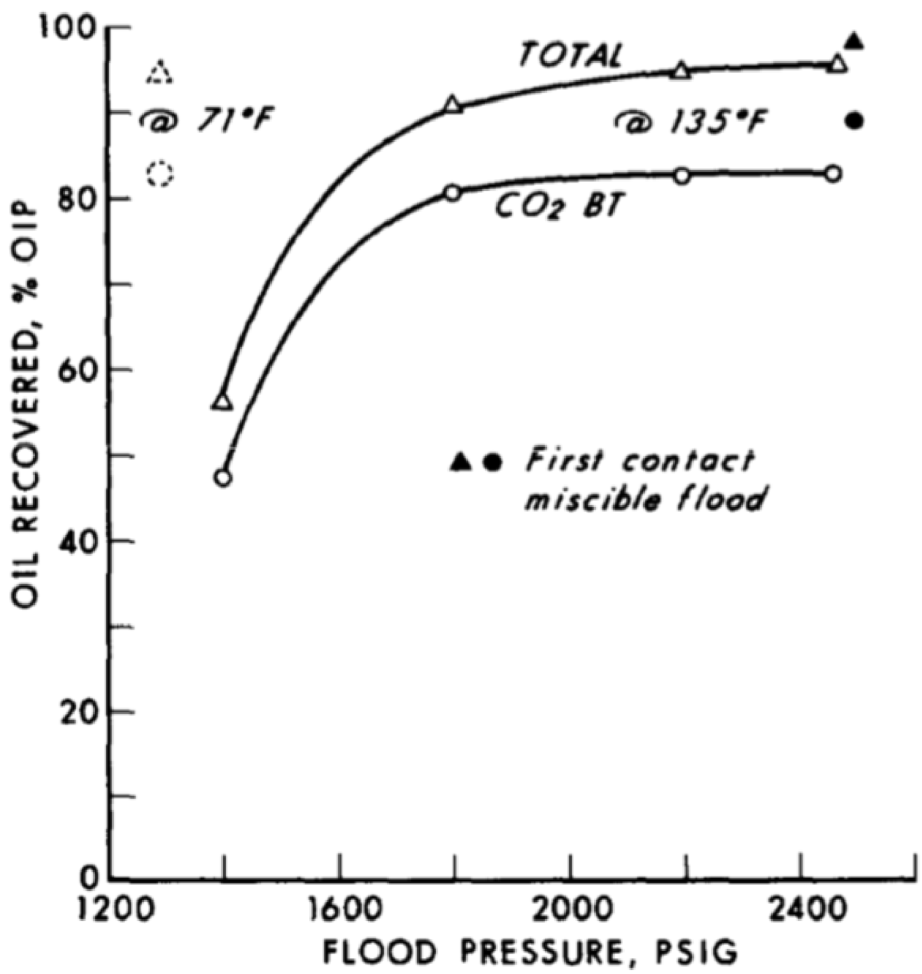

Fig. 3.2—Oil recovered by CO_2 floods under various flooding pressures, at 135°F. The recovery is shown at CO_2 breakthrough and after total CO_2 flood (*Stalkup 1978*).

Past research shows that CO_2 may partially dissolve in the oil while it flows in the reservoir and at the same time extract or vaporize hydrocarbons. These extracted hydrocarbons will enrich the displacing gas front, and at sufficiently high pressure, the enrichment will continue to a level where the gas front composition has been altered significantly, so efficient displacement occurs, which is characteristic for a miscible displacement (Stalkup 1978). This process is effective with CO_2, since it is a much stronger vaporizer of hydrocarbons than natural gas.

Newer studies show that continued contact between oil and CO_2 alters the oil composition until miscibility occurs. The pressure required for miscibility between oil and CO_2 is typically lower than for oil and flue gas, nitrogen or natural gas. In **Fig. 3.3**, oil recovery by CO_2 flooding under different pressures is illustrated, for a West Texas reservoir oil. Recovery from a 42 ft consolidated Boise sandstone and from a 20 ft unconsolidated sand pack were inspected. Above the minimum miscibility pressure (MMP), oil and CO_2 are completely miscible for a fixed temperature, and here, the miscibility pressure is between 1200 to 1300 psi. Fig. 3.3 shows that the oil recovery increases drastically for the cores with increasing pressure, but when the minimum miscibility pressure is reached, very little additional oil will be produced by increasing the pressure further. It should be noted that oil recovery in Fig. 3.3 remained fairly high a few hundred psi below the minimum miscibility pressure, which can be due to low interfacial tension between CO_2-saturated oil and hydrocarbon-enriched CO_2 (Rosman 1977), oil viscosity reduction, vaporization of hydrocarbons and oil swelling (Holm and Josendal 1974). In **Fig. 3.4** results from a similar experiment are shown. In that experiment (Stalkup 1978) used the same oil, the 42 ft consolidated sandstone, but initially the oil was produced by waterflooding. Next, CO_2 was injected to produce the residual oil after waterflooding. As Fig. 3.4 shows, almost 90 % of the residual oil was produced.

The experiments indicate that production under miscible conditions (above minimum miscibility pressure) is more effective than under immiscible conditions, and that large amounts of the residual oil after waterflooding may be produced by CO_2 EOR. Due to the importance of miscibility, minimum miscibility pressure will be discussed next.

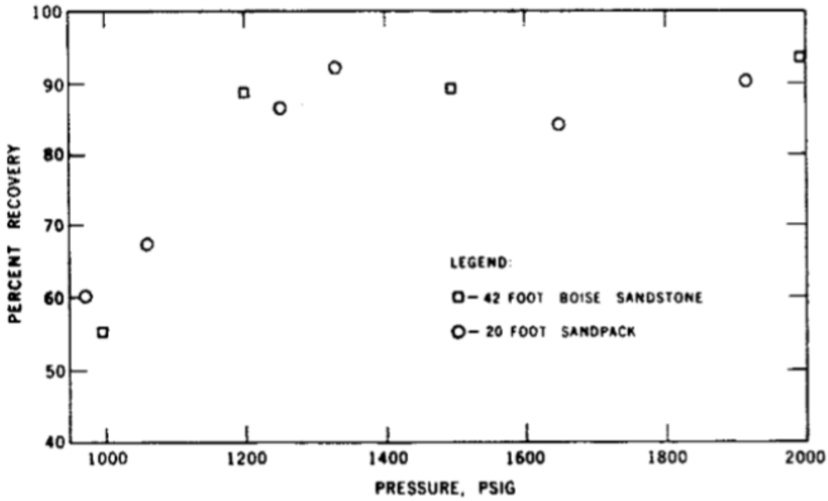

Fig. 3.3—Oil recovery of a West-Texas reservoir oil by CO_2 flooding under various pressures (*Stalkup 1978*).

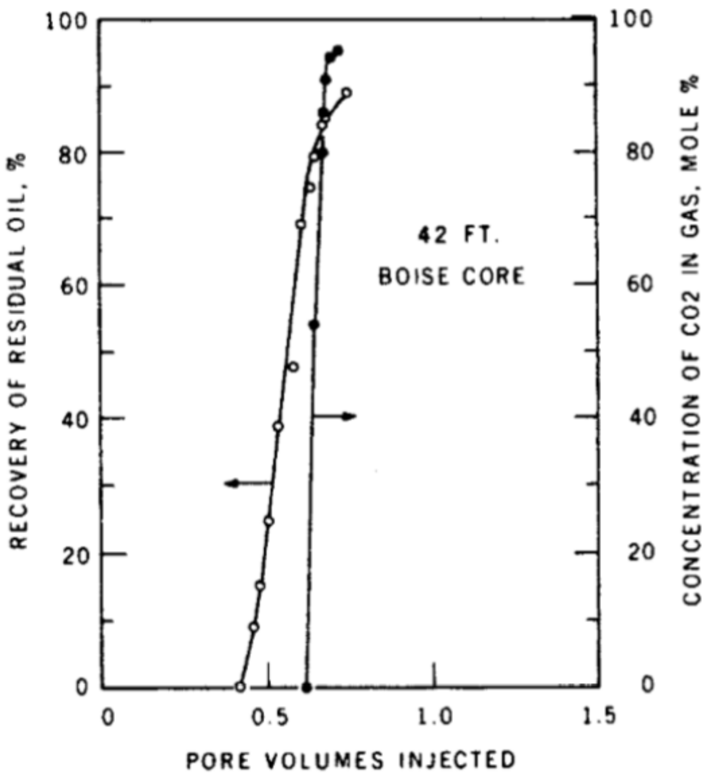

Fig. 3.4—Oil recovery of a West-Texas reservoir oil by CO_2 flooding, after it had been waterflooded until residual oil saturation was reached. Almost 90 % of the residual oil was recovered (*Stalkup 1978*).

3.2.4 Minimum Miscibility Pressure

Above the minimum miscibility pressure (MMP), oil and CO_2 are completely miscible for a fixed temperature. The MMP in a system is dependent on several factors like; oil composition, CO_2 purity and reservoir temperature. The MMP may be increased drastically by small amounts of methane or nitrogen in the CO_2. For the West Texas reservoir oil mentioned in the previous subsection, MMP was approximately 1250 psi when pure CO_2 was injected, but when CO_2 with 15 mol % methane was used, the MMP was increased to 2000 psi. Presence of other components in the CO_2 on the other hand may have a different effect. Ethane and heavier hydrocarbons may decrease the MMP. Oil composition also have typical effects on MMP. Decreased API oil gravity typically increases the MMP. Given that other factors remain the same, increased reservoir temperature typically gives a higher MMP (Stalkup 1978).

Several methods have been proposed to estimate the MMP. A method, that only required API gravity and reservoir temperature, was proposed by NationalPetroleumCouncil (1976), and the method is shown in **table. 3.2**. Another method was proposed by Holm and Josendal (1974), which had both molecular weight of crude oil penthanes and heavier fraction and reservoir temperature as correlation parameters. **Fig. 3.5** shows the accuracy of the two methods, when trying to predict several experimental MMP. The method proposed by NationalPetroleumCouncil (1976) is generally low and often severely inaccurate. Estimates based on the method proposed by Holm and Josendal (1974) is a little off as well, but mostly within 500 psi of experimental data.

Table 3.2—Method proposed by the National Petroleum Council for estimating the minimum miscibility pressure. (*Stalkup 1978*).

Miscibility Pressure vs Gravity

Gravity (°API)	Miscibility Pressure (psi)
<27	4,000
27 to 30	3,000
>30	1,200

Correction for Reservoir Temperature

Temperature (°F)	Additional Pressure Required (psi)
<120	None
120 to 150	+200
150 to 200	+350
200 to 250	+500

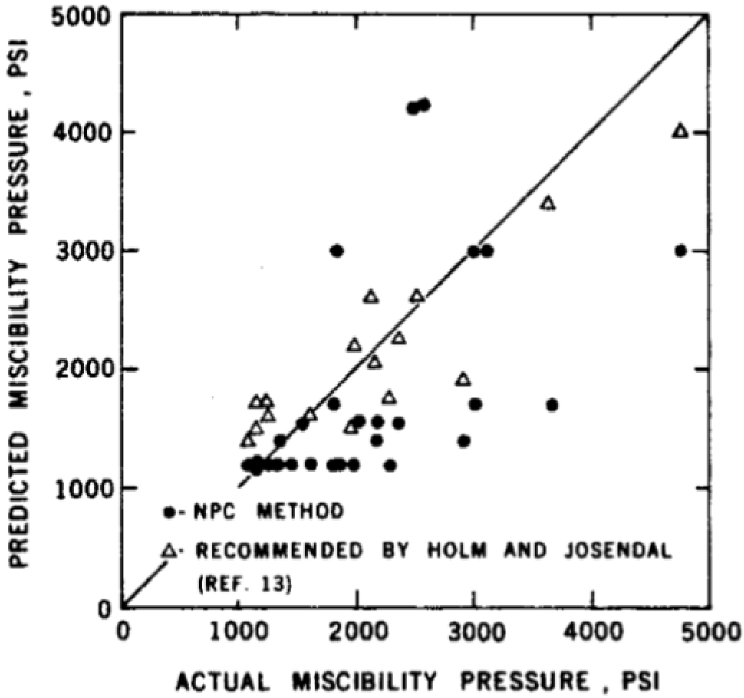

Fig. 3.5—Accuracy of methods proposed to estimate the minimum miscibility pressure. The method proposed by Holm and Josendal seems to agree more with test results, than the method proposed by NPC. (*Stalkup 1978*).

Slim tube experiment is known as the most common method to determine the minimum miscibility pressure. For that method, a long (40-80 ft) high pressure tube with small diameter (0.25 ft) is used. The tube is packed with clean sand or glass beads, so that a fluid permeability of 3-5 Darcys is achieved. Next, it is saturated with the reservoir oil of interest, while reservoir temperature is maintained for the apparatus. Several floods are then performed at various pressures, while the exact composition of displacing CO_2 is injected. The CO_2 may be purified (more than 96 % CO_2) or mixed with other gases. Furthermore, oil recovery versus pressure may be inspected. The lowest pressure where a recovery of 95 % is achieved after 1.3 pore volumes of fluid have been injected, is then the minimum miscibility pressure. For pressures lower than this, the recovery decreases drastically (Holm 1986).

3.2.5 CO_2 EOR in Paleo Residual Oil Zones

Many fields have substantial amounts of oil below the current OWC, which can be a consequence of the OWC moving upwards due to natural water flooding mechanisms over many years. Traditionally, these zones were considered impossible to produce economically, but with modern EOR techniques the zones can be targets for production. Gas injection can be a sensible option, to produce from these zones, called paleo residual oil zones (PROZs).

Comparison of Flue Gas, CO_2 and Methane Injection

Skauge and Surguchev (2000) executed simulations on a reservoir model, to compare effectiveness of injection of CO_2, flue gas and hydrocarbon gas in a PROZ. Their simulations showed that CO_2 injection was much more effective at increasing the oil recovery than flue gas and methane gas injection. They noticed that the oil production rate was 6-8 times as high with CO_2 injection, compared to injection of the two other fluids, and that cumulative oil production naturally was much higher, as illustrated in **Fig. 3.6** and **Fig. 3.7**. Based on results from their simulations, Skauge and Surguchev (2000) concluded that CO_2 injection could be an effective EOR method in the PROZ.

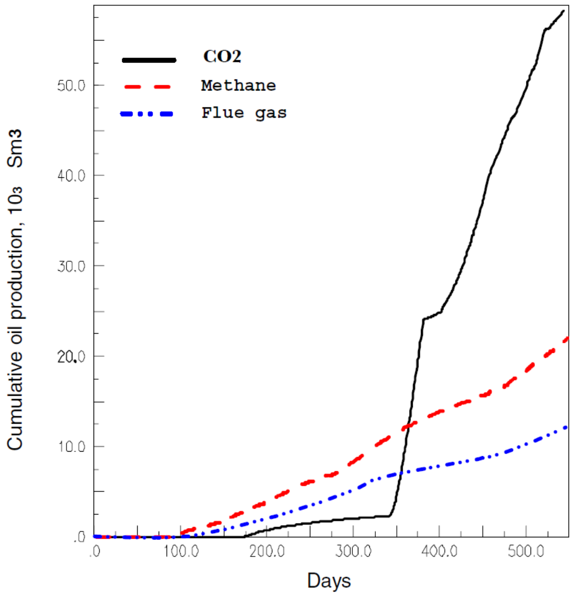

Fig. 3.6—Cumulative oil production in 1000 Sm^3 vs time, in the simulations performed by Skauge and Surguchev (2000). Oil production starts later with CO_2 injection compared to methane and flue gas injection, but the cumulative production is much higher with CO_2 injection (*Skauge and Surguchev 2000*).

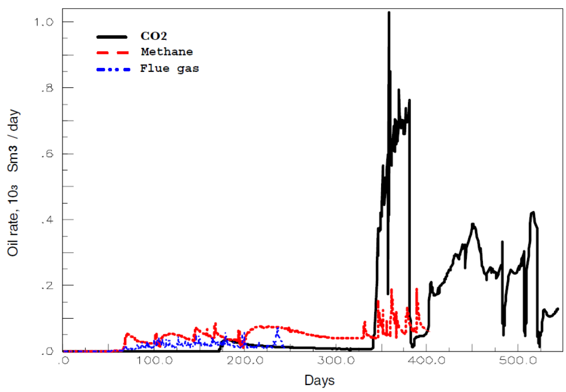

Fig. 3.7—Oil rate in 1000 Sm^3/day vs time, in the simulations performed by Skauge and Surguchev (2000). Oil production starts later with CO_2 injection compared to methane and flue gas injection, but the production rate is much higher with CO_2 injection, when oil production starts. (*Skauge and Surguchev 2000*).

A Laboratory Study

A.A. Aleidan et al. (2014) performed a laboratory study of actual reservoir sponge cores, to investigate the ability of CO_2 to mobilize paleo oil in the PROZ. Their experiments were executed at reservoir conditions, and the cores used were in their native state. They also made sure that selected cores from the MPZ had properties comparable to the cores from the PROZ. They conducted static experiments with a PVT cell, to qualitatively decide if CO_2 would be able to mobilize dead paleo oil. Still images and videos that were taken throughout the experiment showed that the CO_2 managed to mobilize some of the oil. Furthermore, dynamic experiments were performed by coreflooding. Cores from the MPZ and from the PROZ were flooded. According to A.A. Aleidan et al. (2014) it was hard to obtain live reservoir samples from the PROZ, thus the oil in the cores was dead oil. More accurate representation of the PROZ would have been achieved with a live oil, and better mobilization of the oil could have been expected. Their experiments indicated that CO_2 injection had the potential to mobilize paleo oil, but that it might not be as effective as conventional CO_2 injection in the MPZ. They also observed that a soaking period was necessary to mobilize the oil, since the CO_2 then would get time to interact with the paleo oil.

Field Projects

Field projects have been executed to investigate CO_2 EOR in PROZs. In 1991, Shell began a project that was supposed to investigate CO_2 injection in the PROZ in the Wasson Field (Denver Unit). Shell had discovered a thick PROZ under the San Andres reservoir oil column within their Denver Unit in Yoakum County, Texas (Melzer 2006). The saturation in the PROZ was approximately 30 %, which Shell believed was the same as residual oil saturation after waterflooding in the swept portions of the MPZ. CO_2 injection was already conducted in the waterflooded parts of the MPZ to increase the oil recovery, with success. Therefore, Shell had a theory that CO_2 injection could be a reasonable measure to produce oil from the PROZ. Reports about the CO_2 EOR project were limited to internal use, but CO_2 flooding was performed in both the phase 1, phase 2 and phase 3 area. In addition, presentations about the project suggested that production from the PROZs had met their expectation, and further development was planned.

Another field where CO_2 injection has been tested in the PROZ, is the Seminole field (San Andres unit). Amerada Hess was performing CO_2 flooding on that field. Reports about the project has been restricted, but some information was given during the 2001 CO_2 flooding conference in Midland, Texas (Bush 2001). The project had shown positive signs, and expansion of the project was to be expected.

A third CO_2 EOR project in a PROZ was executed in the Wasson field (Bennet Ranch unit). This project was also initiated by Shell, in 1995 (Melzer 2006). A deepening of the wells was planned, to perform CO_2 injection in both the MPZ and the PROZ, but due to low oil prices at the time, that was not carried out. Late in 2003 however, the initial plan of deepening the wells was realized, and CO_2 was injected in both the MPZ and the PROZ in parts of the field. Positive results gave motivation to expand the extent of the project. Furthermore, several other CO_2 EOR in the PROZ projects exist and **table. 3.3** gives an overview of ongoing and planned projects in the Permian basin. Nevertheless, several factors affect whether it can be economically favorable or not.

Table 3.3—Paleo residual oil zone CO_2 EOR projects in the Permian basin (*Harouaka et al. 2013*).

Type & Operator Active CO2 Miscible	Field	State	County	Top MPZ Depth (ft)	Pay zone
Chevron	Vacuum San Andres Grayburg Unit	NM	Lea	4,550	San Andress
Fasken	Hanford	Tex.	Gaines	5,500	San Andres
Hess	Seminole Unit-ROZ Phase 1	Tex.	Gaines	5,500	San Andres
Hess	Seminole Unit-ROZ Phase 2	Tex.	Gaines	5,500	San Andres
Hess	Seminole Unit-ROZ Stage 1 full field	Tex.	Gaines	5,500	San Andres
Hess	Seminole Unit-ROZ Stage 2 full field	Tex.	Gaines	5,500	San Andres
Legado	Goldsmith-Landreth Unit	Tex.	Ector	4,200	San Andres
Occidental	Wasson Bennett Ranch Unit	Tex.	Yoakum	5,250	San Andres
Occidental	Wasson Denver Unit	Tex.	Yoakum	5,200	San Andres
Occidental	Wasson ODC	Tex.	Gaines	5,200	San Andres
XTO/ExxonMobil	Means	Tex.	Andrews	4,500	San Andres

3.3 Challenges and Economics Concerning CO_2 EOR

CO_2 injection can be an effective way of increasing the oil recovery, but there are several challenges that need to be taken into account beforehand, when this EOR method is considered. Deployment limitations are affected by oil composition, depth and temperature of the reservoir, previous oil recovery practices and reservoir features internally that may hinder effective distribution of injected CO_2. Another critical factor decisive for deployment of CO_2 EOR, is the access and proximity to a relatively consistent and pure stream of CO_2 to a low enough price. High costs are related to initiating a CO_2 EOR project and before small fields are able to access a supply, a large nearby anchor field is often needed to develop the infrastructure to deliver CO_2. Furthermore, to produce from a PROZ, CO_2 injection is usually the preferred EOR method and some of the reason to the extensive research and field tests of PROZs in the Permian basin of West Texas is the existence of CO_2 infrastructure including pipelines and processing plants that allow economic delivery and recycling of CO_2.

Implementing a CO_2 EOR project requires several investments. Some of the costs are related to installation of a CO_2 recycle plant and corrosion resistant field production infrastructure and laying CO_2 gathering and transportation pipelines. However, the largest project cost usually is purchase of CO_2 (PTRC 2014). Large investments are needed before the actual CO_2 injection starts and the project potentially starts giving the operator and partners money back. Thus, many companies consider CO_2 EOR a huge risk. To add to that risk, unforeseen heterogeneities in the reservoir or other complications may reduce the potential for increased oil recovery, compared to what had been estimated. Thus, many companies are reluctant to invest in these projects unless nearby CO_2 infrastructure already exists. However, fiscal/tax incentives for CO_2 left and stored in the reservoir may be an extra motivation for companies, given low enough CO_2 prices.

Chapter 4

CO_2 EOR Modeling and Simulation

A reservoir model was constructed by the author. It is a synthetic model, with major simplifications. The model was made to investigate the effect of different parameters in a CO_2 EOR process. Furthermore, simulations were performed on the model, where one parameter at a time was varied so that a sensitivity analysis could be conducted. The simulations were performed in Eclipse, a Schlumberger software.

4.1 Model Description

The reservoir model is a simple box model that initially has as 30 m thick water zone at the bottom, a 20 m thick paleo residual oil zone in the middle and a 50 m thick main pay zone consisting of oil and irreducible water at the top. No gas cap was included, to simplify matters and easier see the effect of injected CO_2. The reservoir is depicted in **Fig. 4.1**. Fig. 4.1 also shows the two wells in the model. In one corner, an injection well is located, while a production well is located in the opposite corner.

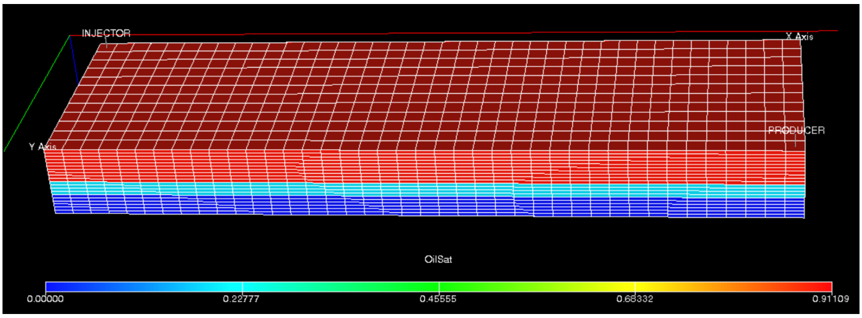

Fig. 4.1—An illustration of the reservoir model used in the simulations. The colors represent initial oil saturation, where blue indicates a low oil saturation and red a high oil saturation. The initial oil saturation in the top zone (MPZ) is 90 %, it is 20 % in the middle zone (PROZ) and 0 % in the bottom zone (water zone). No free gas is present. An injector is shown in the left corner and a producer in the opposite corner (Figure from Flowiz).

The dimensions of the model is (1000x300x100) m, i.e. 1000 m in x-direction, 200 m in y-direction and 100 m in z-direction. Number of cells were set to 40 in x-direction, 12 in y-direction and 20 in z-direction, resulting in 40x12x10 = 9600 grid blocks. All grid blocks had the same dimensions (25x25x5) m. More fluid and rock properties are presented in **table. 4.1**. Rock properties like permeability and porosity are constant throughout the model, meaning that the synthetic reservoir model is homogenous. Furthermore, the permeability is assumed to be isotropic in the model.

Table 4.1—Fluid and rock properties of the synthetic model.

Values given at Reference Pressure = 300 bar		
Reference pressure	300	bar
Property	Value	Unit
Water viscosity	0.305	cP
Oil viscosity	0.601	cP
CO2 viscosity	0.053	cP
Porosity	0.30	fraction
PermX	500	mD
PermY	500	mD
PermZ	500	mD
Formation volume factor water	1.0315	rm3/Sm3
Formation volume factor oil	1.620	rm3/Sm3
Formation volume factor gas	0.00284	rm3/Sm3
Solution gas-oil ration	200	Sm3/Sm3
Connate water saturation	0.10	fraction
Residual oil saturation to water flooding	0.20	fraction
surface oil density	833.9	kg/m3
surface water density	1023.0	kg/m3
surface CO2 density	1.871	kg/m3
Bubble point pressure	251.7	bar

Two vertical wells were introduced to the reservoir model. The injection well was perforated through all the 20 layers in z-direction, while the production well only was perforated in the MPZ. The injection well started out as a water injector, but after approximately nine years, when the oil production rate had fallen to 40 Sm^3/d it was converted to a CO_2 injector in the base case. After CO_2 injection started, the simulation was ran for 5880 more days, or 16.1 years.

Reservoir models are used by companies to help decide optimal well locations, anticipate production, indicate the performance of different production strategies and more. Since a good model and information about the reservoir in general can be decisive for decisions about the field development, vast amounts of money are spent to gather data about the reservoir. The information is acquired through seismic, core analysis, log interpretation, well tests or other methods. Thus, relatively realistic models may be constructed and as more test data or production data is gathered, the models may be updated in a process called history matching to make the model more realistic. Yet, these models are never able to exactly predict the reservoir behavior, since uncertainties are related to the obtained data and the data rarely is conclusive. In addition, data is only gathered from a small fraction of the reservoir and when the whole reservoir is supposed to be modeled based on that information, assumptions must be made and heterogeneities are tough to capture. Nevertheless, models can be useful and good enough to estimate typical behavior of a reservoir.

The reservoir model constructed for use in this thesis does not represent a specific real reservoir, meaning that it mostly is not based on data from a field. Major simplifications were made in the model, compared to what often are seen in more advanced commercial models used by companies. Considering the fact that even those models are uncertain and have limitations it becomes clear that the model used in this thesis, which is more simplified than commercial models, has limitations. However, much like many commercial models, this simplified model is advanced enough to serve its purpose. The model is not entirely based on data from a real field, however, measures were made to make the model simple, yet realistic enough to investigate CO_2 EOR. PVT data and relative permeabilities in the model were taken from a real field, with a paleo residual oil zone, where CO_2 injection had been executed. In that field, the paleo oil and MPZ oil were assumed to have similar properties and the same assumption was made for the model in this thesis. CO_2 injection rate in the base case was set to 1 500 000 Sm^3/d which is a feasible injection rate, if access and proximity to a relatively consistent and pure stream of CO_2 to a low enough price may be achieved. Also, with an injection rate like that, CO_2 injection had a significant impact on the oil production. Hence, importance of different parameters was assumed to become evident during the sensitivity analysis to come, as sharp changes were expected. The preceding water injection had an injection rate to match the following CO_2 injection rate in reservoir volume. This was done by estimating reservoir volume of injected gas with Eq. 4.1, where surface volume was known and a gas formation volume factor at average reservoir pressure during CO_2 injection, was used. An iterative process was needed to find the reservoir pressure during CO_2 injection after water injection had been conducted. When the injected CO_2 reservoir volume rate had been found, Eq. 4.1 was manipulated to find the surface injection rate of water. Formation volume factor of water was known and reservoir injection rate of water was equal to reservoir injection rate of CO_2.

$$V_{n_{res}} = B_n V_{n_{surf}}, \quad \text{...} \quad (4.1)$$

Where:
$V_{n_{res}}$ = reservoir volume of fluid n [rm^3]
B_n = formation volume factor of fluid n [rm^3/Sm^3]
$V_{n_{surf}}$ = surface volume of fluid n [Sm^3]

The water injection rate necessary to match CO_2 injection rate was equal to 4140 Sm3/d and was evaluated to be feasible, considering typical water injection rates in commercial fields. Furthermore, the well locations (on opposite sides) were chosen to easily see how oil was swept by the moving front. Thickness of the paleo residual oil zone relative to the MPZ was not based on a specific field, but it was inspired by real observations. PROZ thickness/MPZ thickness vary from field to field and the ratio may have a broad range and even vary within a field. Nevertheless, the PROZ needs to have a considerable thickness to be relevant for EOR projects.

Due to injected fluids, a pressure gradient will occur over the reservoir. This pressure gradient will mainly depend on injection rate, production rate, permeability and distance between the wells. To avoid a large peak in the production due to a much lower bottomhole pressure (BHP), and to get a stable pressure gradient over the reservoir relatively quickly, the oil production rate was controlled by a minimum bottomhole pressure close to the (3 bar below) initial reservoir pressure. A maximum production rate was also used, but with the given injection rates and high minimum bottomhole pressure, minimum bottomhole pressure was the controlling element. Hence, the high minimum BHP was chosen to quickly achieve steady state and simplify the process of interpreting results.

4.2 Eclipse 100 Miscible Flood Modeling

To model the mixing of injected CO_2 and oil, Eclipse's MISCIBLE keyword, which enables a miscible flood model, was used. The MISCIBLE keyword in Eclipse requests a different treatment of miscibility in Eclipse 100 (black oil) compared to Eclipse 300 (compositional model). Eclipse 100 was used for this thesis and will therefore be focused on. The miscible flood modeling in Eclipse 100 employs a mixing parameter called Todd-Longstaff parameter to model miscibility in a three-component system. The three components in the model is reservoir oil, injected gas (CO_2 in this case) and water. The injected CO_2 and reservoir oil components are assumed to be miscible in all proportions and therefore, only one hydrocarbon phase exists in the reservoir. The hydrocarbon phase consists of oil with solution gas and injected CO_2 (Schlumberger 2016). Modification of the standard density and viscosity calculations in a black oil simulator is performed when the Todd-Longstaff mixing parameter is used.

Physical dispersion between the miscible components in the hydrocarbon phase is treated empirically by the Todd-Longstaff model. An empirical parameter, ω, with value between 0 and 1 is introduced. ω represents size of the dispersed zone in each grid block and therefore controls the degree of mixing within each block. If $\omega = 1$, the injected CO_2 and oil are fully mixed within each block. With $\omega = 0$, the miscible components will have a negligible dispersed zone between them and the components will have density and viscosity of pure components. To model real field situations an ω value between 0 and 1 is often used to replicate incomplete mixing of the miscible components (Schlumberger 2016).

There is only one hydrocarbon phase in the reservoir, consisting of the two miscible components, injected gas and oil. A water phase is also present in the reservoir. Thus, the flow has two-phase characteristics, with the hydrocarbon phase and water as the two flowing phases. Therefore, two-phase relative permeability curves are needed as input to the model. Relative permeability curves are needed for the water as a function of water saturation, $k_{rw}(S_w)$ and for the hydrocarbon phase as a function of hydrocarbon saturation, $k_{rn}(S_n)$, where S_w is the water saturation and S_n is the hydrocarbon saturation, i.e. saturataion of injected gas plus saturation of oil, $S_o + S_g$. Relative permeability of injected gas and oil are then calculated as saturation weighted fraction according to Eq. 4.2. and Eq. 4.3 (Schlumberger 2016):

$$k_{rg} = \frac{S_g - S_{gc}}{S_n - S_{gc} - S_{or}} k_{rn}(S_n), \quad \ldots\ldots\ldots\ldots\ldots\ldots \quad (4.2)$$

$$k_{ro} = \frac{S_o - S_{or}}{S_n - S_{gc} - S_{or}} k_{rn}(S_n), \quad \ldots\ldots\ldots\ldots\ldots\ldots \quad (4.3)$$

where,

k_{rg} = relative permeability of miscbible gas [-]

k_{ro} = relative permeability of miscbible oil [-]
k_{rn} = relative permeability of hydrocarbon phase [-]
S_n = saturation of hydrocarbon phase [-]
S_g = saturation of gas [-]
S_o = saturation of oil [-]
S_{gc} = critical gas saturation [-]
S_{or} = residual oil saturation [-]

The mixture viscosity is given by a fluid mixing rule shown in Eq. 4.4, while the effective gas and oil viscosities are given by Eq. 4.6 and Eq. 4.5 (Schlumberger 2016):

$$\mu_m = \frac{\mu_o \mu_g}{(\frac{S'_g}{S'_n}\mu_o^{1/4} + \frac{S'_o}{S'_n}\mu_g^{1/4})^4}, \quad (4.4)$$

$$\mu_{o_{eff}} = \mu_o^{1-\omega}\mu_m^{\omega}, \quad (4.5)$$

$$\mu_{g_{eff}} = \mu_g^{1-\omega}\mu_m^{\omega}, \quad (4.6)$$

where,
μ_m = mixture viscosity [cP]
μ_o = oil viscosity [cP]
μ_g = gas viscosity [cP]
S'_o = S$_o$ - S$_{or}$ [-]
S'_g = S$_g$ - S$_{gc}$ [-]
S'_n = S$'_o$ - S$'_g$ [-]
$\mu_{o_{eff}}$ = effective oil viscosity [cP]
$\mu_{g_{eff}}$ = effective gas viscosity [cP]

Both of the effective viscosities are equal to the mixture viscosity if $\omega = 1$. This case is treated as a local unit mobility ratio displacement by the Todd-Longstaff model. "An ω value equal to 0 demonstrates a fully segregated case with a local high adverse, mobility ratio displacement and a negligibly thin oil-gas dispersed zone" (Schlumberger 2016). A partial mixing zone may be modeled by an intermediate value of ω.

The same quarter power rule principle applies in the process of calculating the effective densities as for the effective viscosities. The same Todd-Longstaff mixing parameter, ω, as was used for the viscosities, will be used by default for the densities. However, a different Todd-Longstaff mixing parameter may be defined for the densities, if that is reasonable. First, effective saturation fractions are calculated by Eq. 4.7 and Eq. 4.8. Next, the effective oil and gas densities are calculated by Eq. 4.9 and Eq. 4.10 (Schlumberger 2016)

$$(\frac{S_o}{S_n})_{oe} = \frac{\mu_o^{1/4}(\mu_{o_{eff}}^{1/4} - \mu_g^{1/4})}{\mu_{o_{eff}}^{1/4}(\mu_o^{1/4} - \mu_g^{1/4})}, \quad \text{..................................} \quad (4.7)$$

$$(\frac{S_o}{S_n})_{ge} = \frac{\mu_o^{1/4}(\mu_{g_{eff}}^{1/4} - \mu_g^{1/4})}{\mu_{g_{eff}}^{1/4}(\mu_o^{1/4} - \mu_g^{1/4})}, \quad \text{..................................} \quad (4.8)$$

$$\rho_{o_{eff}} = \rho(\frac{S_o}{S_n})_{oe} + \rho_g[1-(\frac{S_o}{S_n})_{oe}], \quad \text{................................} \quad (4.9)$$

$$\rho_{g_{eff}} = \rho(\frac{S_o}{S_n})_{ge} + \rho_g[1-(\frac{S_o}{S_n})_{ge}], \quad \text{...............................} \quad (4.10)$$

where,
$(\frac{S_o}{S_n})_{oe}$ = effective saturation fraction for oil density calucations [-]
$(\frac{S_o}{S_n})_{ge}$ = effective saturation fraction for gas density calucations [-]
$\rho_{o_{eff}}$ = effective oil density [kg/m^3]
$\rho_{g_{eff}}$ = effective gas density [kg/m^3]
ρ_o = pure oil density [kg/m^3]
ρ_g = pure gas density [kg/m^3]

Similar to the viscosities, the effective densities are equal to each other in the case of full mixing, where $\omega = 1$. If $\omega = 0$, the effective densities are equal to their respective "pure" phase densities ($\rho_{o_{eff}} = \rho_o$ and $\rho_{g_{eff}} = \rho_g$).

It might be counterintuitive to say that there only is one hydrocarbon phase and still compute distinct properties for oil and the injected gas. However, this is because despite the fluids being miscible, the oil and gas components will still exist as distinct components within one hydrocarbon phase, and Eclipse 100 calculates properties for each component. Computations are performed continuously and grid blocks that have an injected gas saturation equal to critical gas saturation and a high oil saturation will have a hydrocarbon phase with oil properties. If the oil saturation in a grid block is equal to residual oil saturation and gas saturation is high, the hydrocarbon phase in that grid block will have gas properties. In grid blocks with mobile oil and mobile gas, the hydrocarbon phase will have a mix of injected gas and oil properties. The Todd-Longstaff mixing parameter controls degree of mixing within each grid block and a low value may be used to capture viscous fingering effects.

4.3 Construction of a Base Case and Sensitivity Analysis

In many cases where a sensitivity analysis is performed, a base case is decided beforehand based on real data from a specific field and previous production routines if available. In this thesis a synthetic model was utilized, and data solely from one specific field was not used. However, the goal was not to optimize the production strategy in a specific field, but rather see the effect of essential parameters. Hence, a base case needed to be constructed. In the construction of a base case, two important principles were focused on. The base case needed to be simple enough to easily interpret the results as parameters were varied later. Secondly, it needed to be realistic enough, so that the results could be compared to a real scenario on a general level.

Decisions on well locations and perforation intervals were explained in section 4.1 and so was water and CO_2 injection rates and time of CO_2 injection start as well. CO_2 injection could have been conducted from the beginning, but since it often is preceded by water injection until an uneconomic oil production rate is reached, that was done in this study too. The Todd-Longstaff mixing parameter, ω, was set to a value of 0.95 in the base case. This was because it has been observed that high values of the parameter often give results similar to what is achieved when conducting miscible flooding in a compositional model (Eclipse 300). Residual oil saturation after CO_2 flooding was controlled by the ECLIPSE keyword SORWMIS and was set to 0.03, as the residual oil saturation was assumed to be low with miscible CO_2 flooding. Injection start of CO_2 was set to 3296 days (9.03 years) and CO_2 injection rate was set equal to 1 500 000 Sm^3/d as explained in section 4.1. The four parameters to be varied one by one in the sensitivity analysis were; 1. CO_2 injection start, 2. CO_2 injection rate, 3. Residual oil saturation after miscible CO_2 injection (SORWMIS), 4. Todd-Longstaff mixing parameter (TLMIXPAR). The value of those four parameters in the base case are summarized in **table. 4.2**. The values of the parameters during the sensitivity analysis are shown in **table. 4.3** to **table. 4.6**. When one parameter was changed, all other parameters were kept constant at base case values, to easily see the significance of a parameter. All results when changing a parameter was compared to the base case and a case where water injection was performed from start to finish, i.e. until CO_2 injection finished in the base case.

Table 4.2—Value of the parameters to be varied, in the base case.

Base case		
Parameter	Value	Unit
CO2 injection start	3296	days
CO2 injection rate	1 500 000	Sm3/d
TLMIXPAR	0.95	[-]
SORWMIS	0.03	[-]

Table 4.3—CO2 injection rate sensitivity runs.

Rate sensitivity			
Sensitivity nr.	Parameter	Percentage of base case	Unit
1	CO2 injection rate	10	%
2	CO2 injection rate	25	%
3	CO2 injection rate	50	%
4	CO2 injection rate	125	%
5	CO2 injection rate	200	%

Table 4.4—CO2 injection start sensitivity runs.

CO2 injection start sensitivity			
Sensitivity nr.	Parameter	Value	Unit
1	CO2 injection start after	0	days
2	CO2 injection start after	716	days
3	CO2 injection start after	1101	days
4	CO2 injection start after	2420	days
5	CO2 injection start after	4464	days

Table 4.5—TLMIXPAR sensitivity runs.

TLMIXPAR sensitivity			
Sensitivity nr.	Parameter	Value	Unit
1	TLMIXPAR	0.0	[-]
2	TLMIXPAR	0.3	[-]
3	TLMIXPAR	0.5	[-]
4	TLMIXPAR	0.7	[-]
5	TLMIXPAR	0.9	[-]
6	TLMIXPAR	1.0	[-]

Table 4.6—SORWMIS sensitivity runs.

SORWMIS sensitivity			
Sensitivity nr.	Parameter	Value	Unit
1	SORWMIS	0.0	[-]
2	SORWMIS	0.08	[-]
3	SORWMIS	0.15	[-]
4	SORWMIS	0.20	[-]

4.4 Limitations

A limitation of the synthetic model in this thesis is the homogeneity. Real reservoirs will have more complex structures and a varying degree of heterogeneity. When neglecting heterogeneities some effects are lost. Thief zones may for example cause the injected CO_2 to flow only in a small part of the reservoir, leaving large amounts of oil behind. Other changes of properties within the reservoir may affect sweep efficiency and oil production. In some cases, variations of wettability, which affects capillary pressure and relative permeability, may for example be significant.

Another limitation with the simulations, is that a black oil model has been used instead of a compositional model. With a compositional model it is easier to take the oil composition into account, since it may be divided into user defined components and Eclipse 300 will do calculations for all the components. Component exchange between injected CO_2 and the oil is easier modeled with a compositional model. In immiscible flow, for example for a low reservoir pressure, CO_2 and oil do not mix well and one might think that the CO_2 injection will not increase the oil production considerably. However, even with immiscible flow, CO_2 may transport large amounts of oil through component exchange. In that process, some of the light to intermediate components of the oil are transferred to the CO_2 phase and flows easily with the CO_2 towards production wells. When using a black oil model this effect is hard to capture, since the oil only is considered as one component which has a type of average properties of all the components within it.

Assumption of similar oil in the main pay zone and paleo residual oil zone is also a limiting aspect for the model. As A. Aleidan et al. (2017) studies showed, these oils might be different despite seemingly looking the same and having the same source rock. The differences might not be spotted until inspections on molecular level is conducted. A. Aleidan et al. (2017) concluded that the differences spotted when doing so, might be significant enough to affect choice of EOR method or production strategy.

Three limitations of the synthetic model have been pointed out and the lack of real field data has already been mentioned. Nonetheless, the two principles of making the model simple and realistic enough are still valid. The Todd-Longstaff is an empirical parameter, that can be varied to account for oil compositional effects, geometrical effects og heterogeinities. It may also be used to control the sweep efficiency, as it affects mobility ratio. Hence, in the lack of a compositional model, miscibility treatment by the Todd-Longstaff parameter may be a reasonable approximation. It may also be a reasonable choice, as it less computational heavy than simulations with a composition model, and therefore takes less time and costs less money. The assumption of similar paleo oil and MPZ oil is not correct for all fields, as pointed out by A. Aleidan et al. (2017). However, it might be a good estimation in some fields. This has for instance been observed in some of the fields in the North Sea. Furthermore, the model has limitations, but it is still sensible enough to serve its purpose and qualitatively asses the effect of different parameters.

Chapter 5

Results

All results were obtained from simulations performed on the synthetic box model. Effect of injected CO_2 on the oil production was inspected. Oil recovery from the main pay zone and from the paleo residual oil zone were investigated distinctively. The focus was on the significance of various parameters, namely CO_2 injection start, CO_2 injection rate, Todd-Longstaff mixing parameter and miscible residual oil saturation (oil saturation after injection of CO_2). The focus is reflected by the plots in this chapter. Sensitivity analysis of the four mentioned parameters are presented. For all sensitivities, oil recovery factor of the MPZ, oil recovery factor of the paleo residual oil zone, oil production rate of the field and cumulative oil production of the field are presented. Thorough economic analysis was outside the scope of the studies conducted with the box model. If quantitative economic analysis were to be executed, plots of the cumulative oil production would have been essential, together with plots of the water cut and GOR. In addition, separation, compression, processing, facilty and other costs would be decisive. However, this was not central for the studies as qualitative assessment of parameter importance was the main objective. Yet, significance of GOR and water cut is briefly discussed in section 6.5.

5.1 CO_2 Injection Rate Sensitivity

Fig. 5.1, **Fig. 5.2**, **Fig. 5.3** and **Fig. 5.4** show the impact of CO_2 injection rate on the oil production rate of the field, cumulative oil production of the field, recovery factor of the MPZ, and recovery factor of the PROZ respectively. In each plot, seven different graphs are included. One graph for the case of water being injected throughout the simulation. One graph for the base case, where all parameters are as in table. 4.2. Five graphs where all parameters were being kept constant at base case values, except the CO_2 injection rate, which was different in all the five cases. Generally, it can be observed that the oil production increases with increasing CO_2 injection rate.

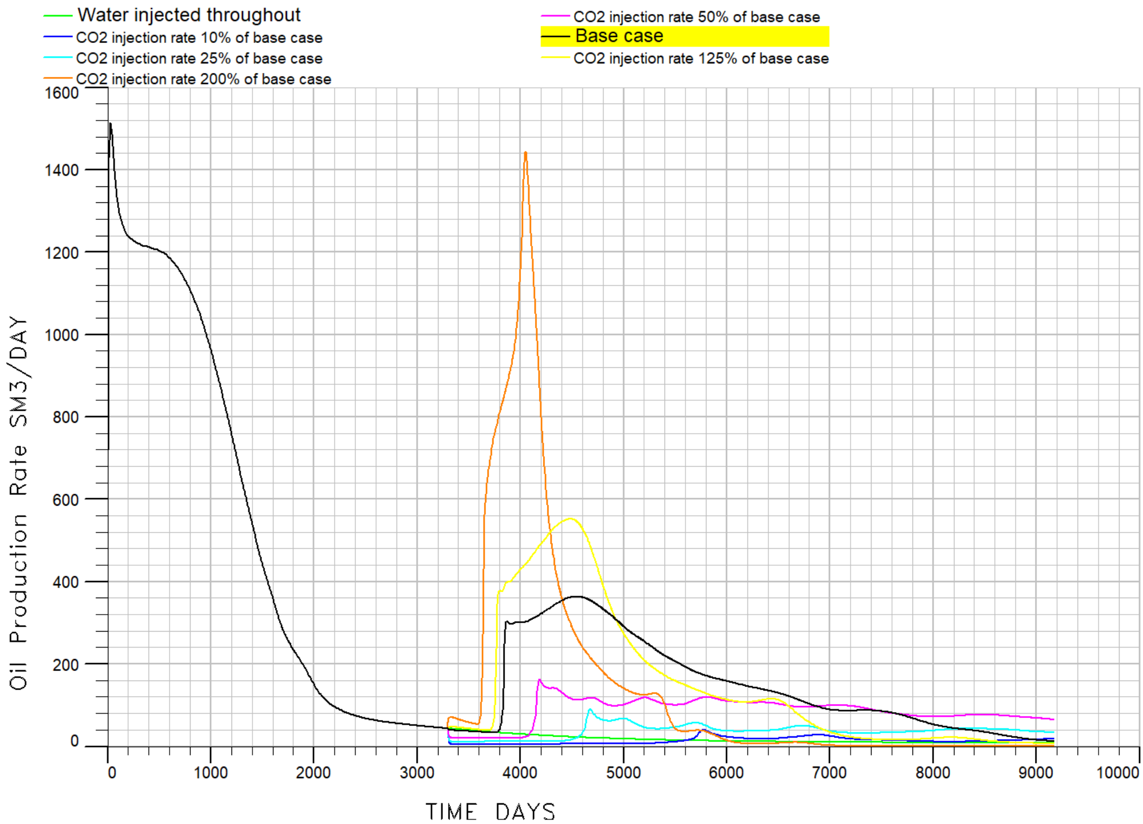

Fig. 5.1—Effect of CO_2 Injection Rate on Oil Production Rate. Oil production rate is plotted versus time, for different CO_2 injection rates. The seven scenarios plotted are the; base case (black), water injected throughout(green), CO_2 injection rate = 10 % of base case (blue), CO_2 injection rate = 25 % of base case (turquoise), CO_2 injection rate = 50 % of base case (purple), CO_2 injection rate = 125 % of base case (yellow), CO_2 injection rate = 200 % of base case (orange) (*figure from Office in the Schlumberger simulation launcher*).

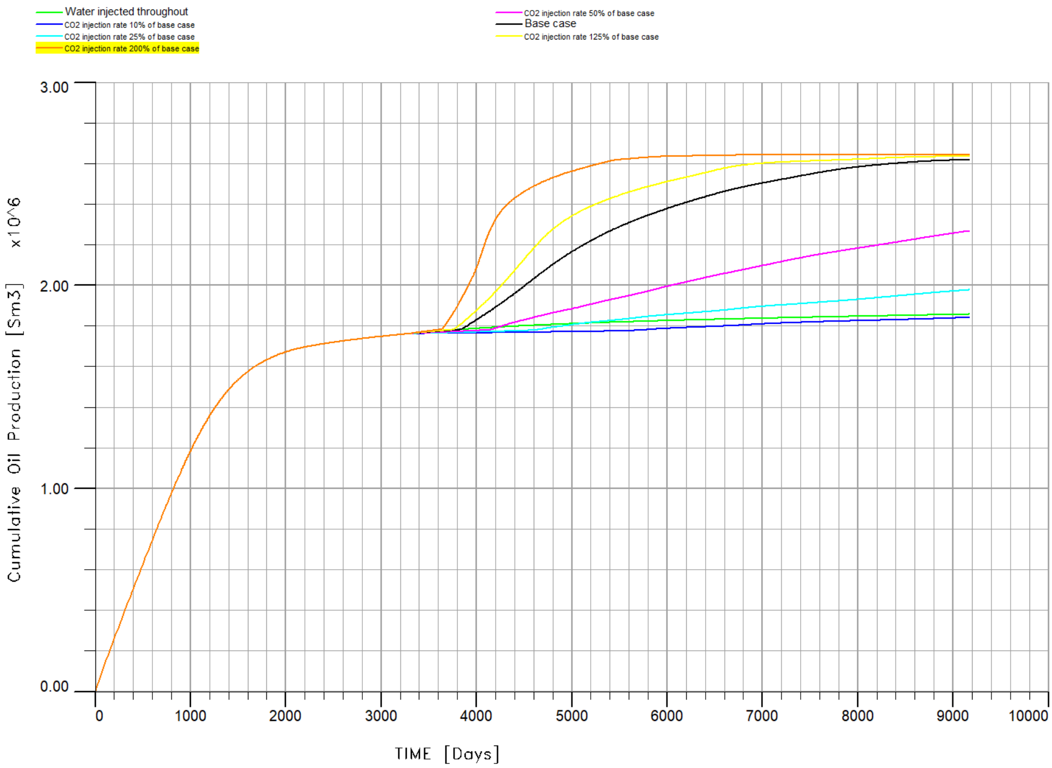

Fig. 5.2—Effect of of CO_2 injection rate on cumulative oil production. Cumulative oil production is plotted versus time, for different CO_2 injection rates. The seven scenarios plotted are the; base case (black), water injected throughout(green), CO_2 injection rate = 10 % of base case (blue), CO_2 injection rate = 25 % of base case (turquoise), CO_2 injection rate = 50 % of base case (purple), CO_2 injection rate = 125 % of base case (yellow), CO_2 injection rate = 200 % of base case (orange) (*figure from Office in the Schlumberger simulation launcher*).

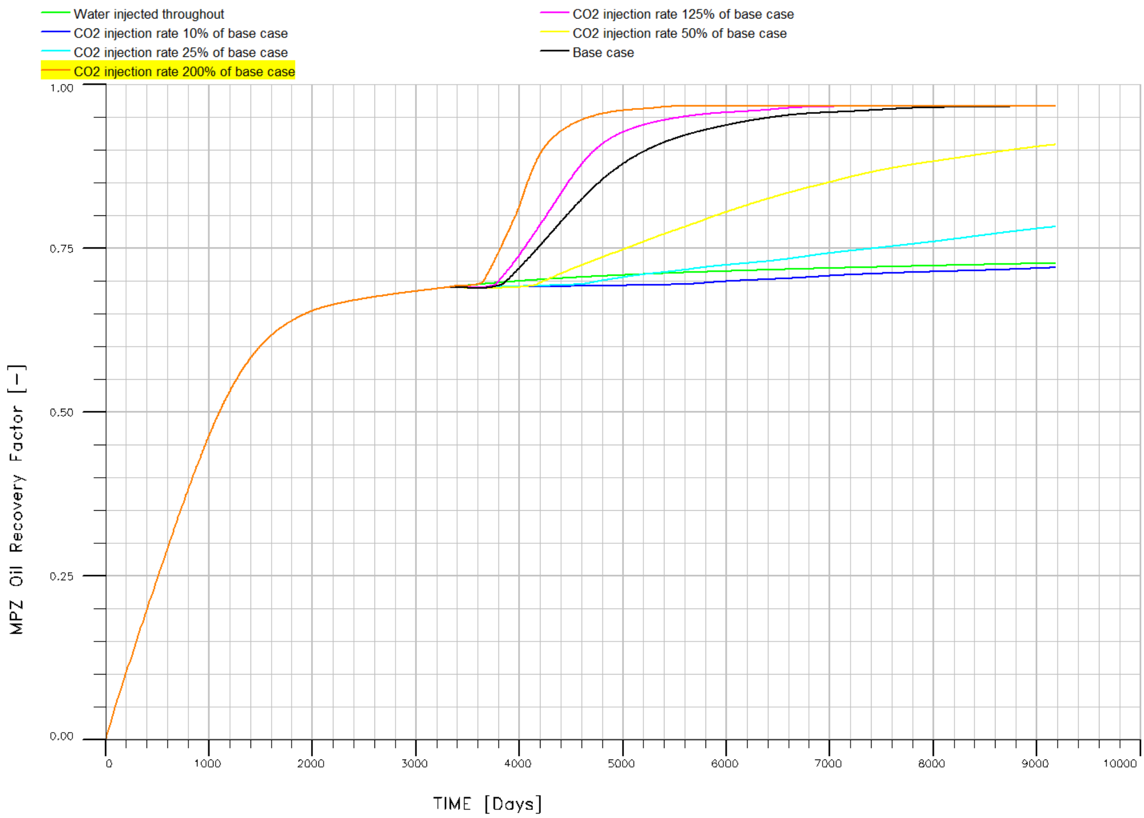

Fig. 5.3—Effect of of CO_2 injection rate on MPZ oil recovery factor. MPZ oil recovery factor is plotted versus time, for different CO_2 injection rates. The seven scenarios plotted are the; base case (black), water injected throughout(green), CO_2 injection rate = 10 % of base case (blue), CO_2 injection rate = 25 % of base case (turquoise), CO_2 injection rate = 50 % of base case (yellow), CO_2 injection rate = 125 % of base case (purple), CO_2 injection rate = 200 % of base case (orange) (*figure from Office in the Schlumberger simulation launcher*).

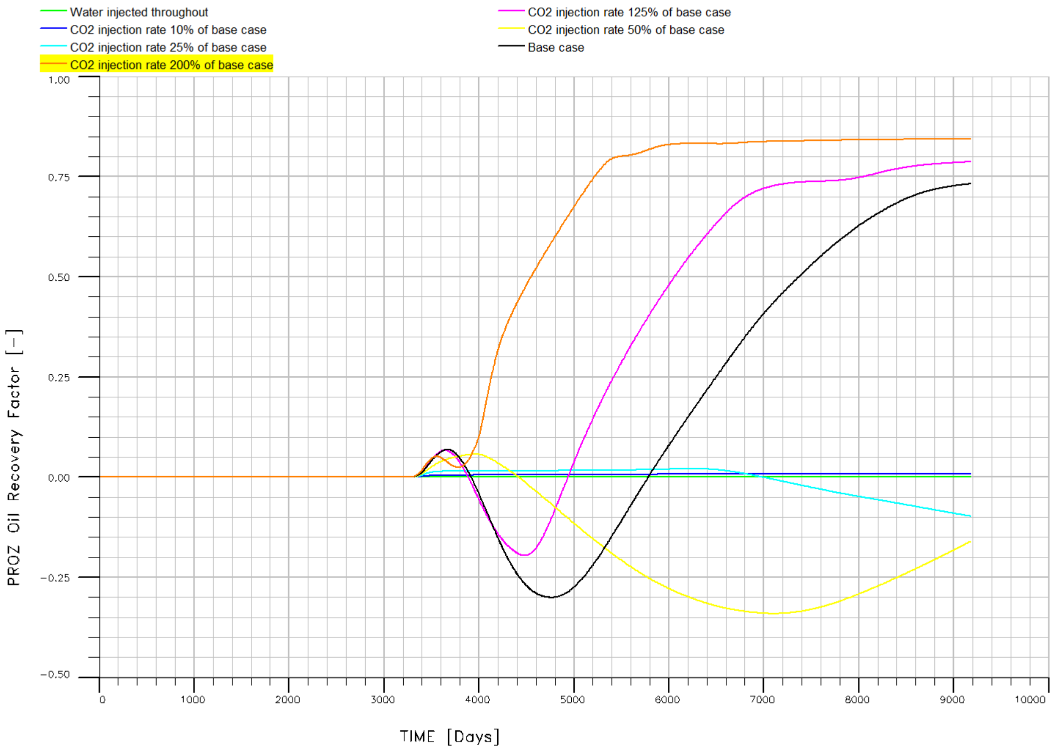

Fig. 5.4—Effect of CO_2 injection rate on PROZ oil recovery factor. PROZ oil recovery factor is plotted versus time, for different CO_2 injection rates. The seven scenarios plotted are the; base case (black), water injected throughout(green), CO_2 injection rate = 10 % of base case (blue), CO_2 injection rate = 25 % of base case (turquoise), CO_2 injection rate = 50 % of base case (yellow), CO_2 injection rate = 125 % of base case (purple), CO_2 injection rate = 200 % of base case (orange) (*figure from Office in the Schlumberger simulation launcher*).

5.2 Effect of CO_2 Injection Start Time

Fig. 5.5, **Fig. 5.6**, **Fig. 5.7** and **Fig. 5.8** show the impact of CO_2 injection start on the oil production rate of the field, cumulative oil production of the field, recovery factor of the MPZ, and recovery factor of the PROZ respectively. In each plot, seven different graphs are included. One graph for the case of water being injected throughout the simulation. One graph for the base case, where all parameters are as in table. 4.2. Five graphs where all parameters were being kept constant at base case values, except the CO_2 injection start time, which was different in all the five cases.

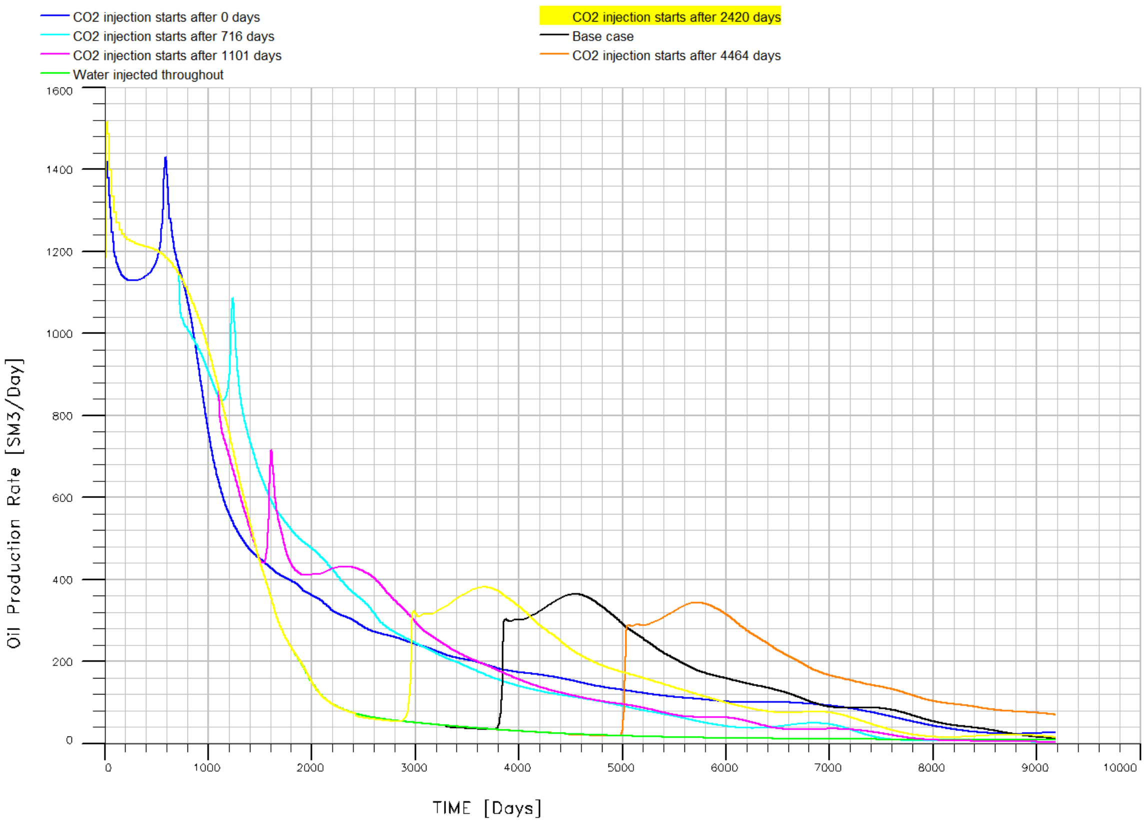

Fig. 5.5—Effect of CO_2 injection start on oil production rate. Oil production rate is plotted versus time, for different CO_2 injection start times. The seven scenarios plotted are the; base case (black), water injected throughout(green), CO_2 injection start after 0 days (blue), CO_2 injection start after 716 days (turquoise), CO_2 injection start after 1101 days (purple), CO_2 injection start after 2420 days (yellow), CO_2 injection start after 4464 days (orange) (*figure from Office in the Schlumberger simulation launcher*).

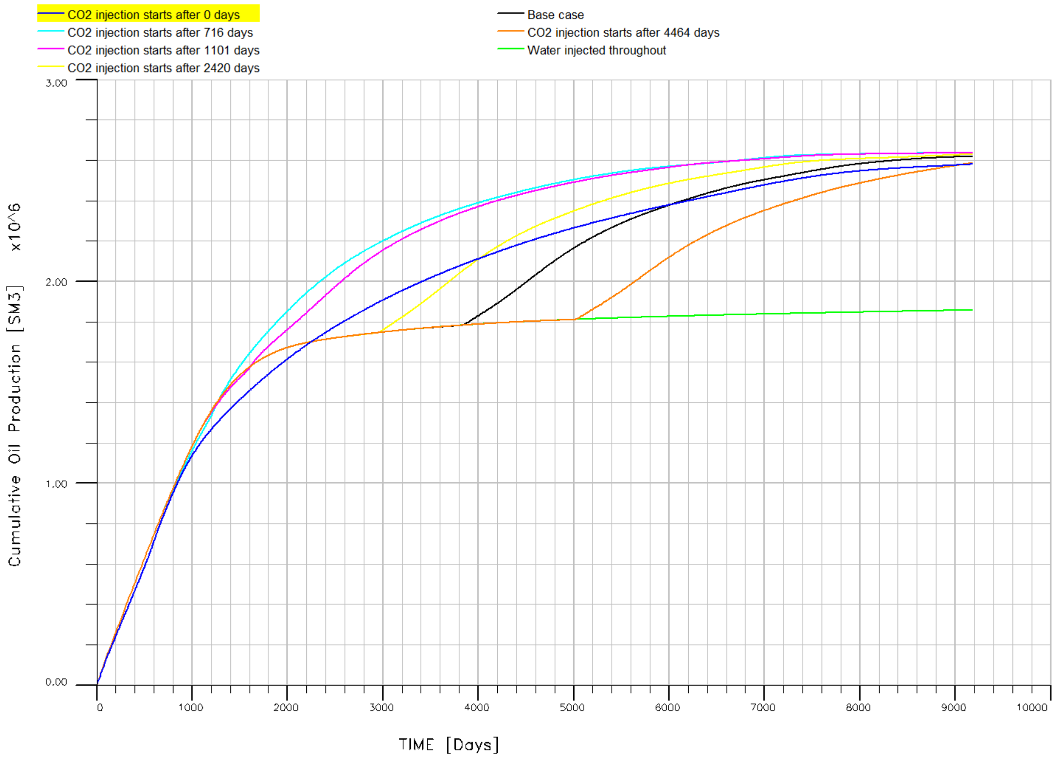

Fig. 5.6—Effect of of CO_2 injection start time on cumulative oil production. Cumulative oil production is plotted versus time, for different CO_2 injection start times. The seven scenarios plotted are the; base case (black), water injected throughout(green), CO_2 injection start after 0 days (blue), CO_2 injection start after 716 days (turquoise), CO_2 injection start after 1101 days (purple), CO_2 injection start after 2420 days (yellow), CO_2 injection start after 4464 days (orange) (*figure from Office in the Schlumberger simulation launcher*).

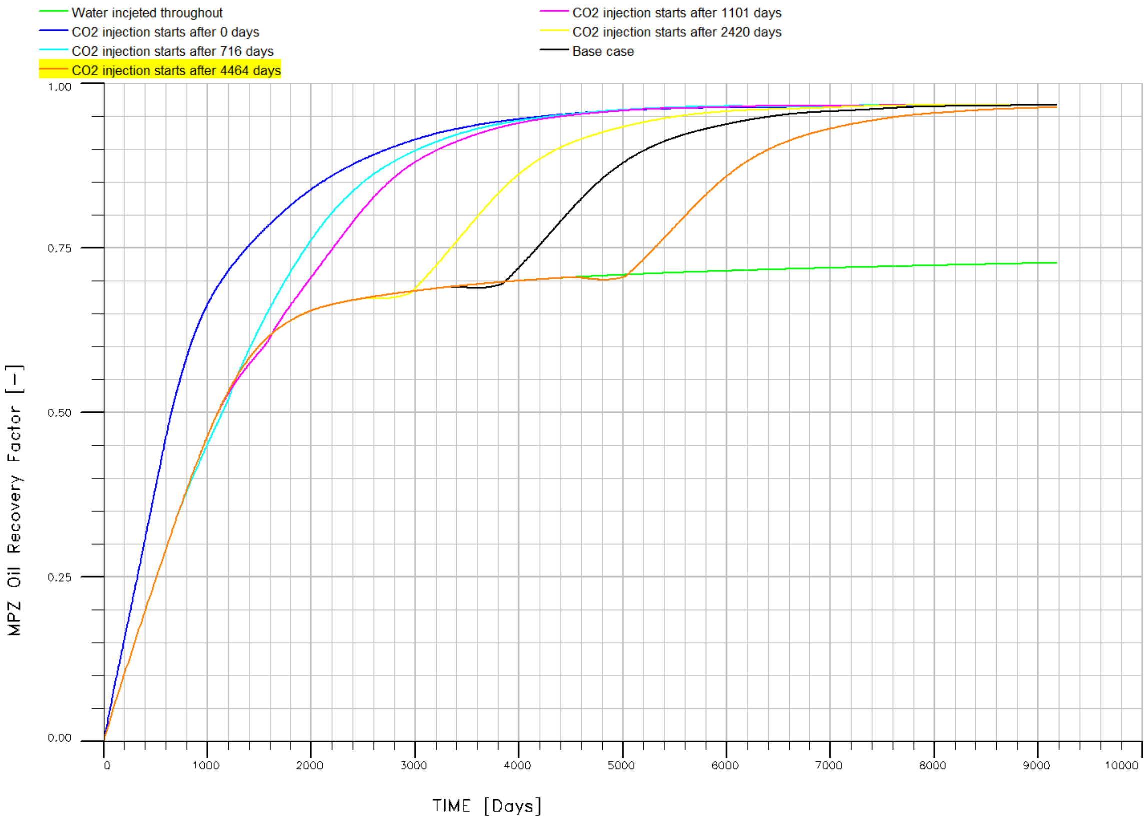

Fig. 5.7—Effect of of CO_2 injection start time on MPZ oil recovery factor. MPZ oil recovery factor is plotted versus time, for different CO_2 injection start times. The seven scenarios plotted are the; base case (black), water injected throughout(green), CO_2 injection start after 0 days (blue), CO_2 injection start after 716 days (turquoise), CO_2 injection start after 1101 days (purple), CO_2 injection start after 2420 days (yellow), CO_2 injection start after 4464 days (orange) (*figure from Office in the Schlumberger simulation launcher*).

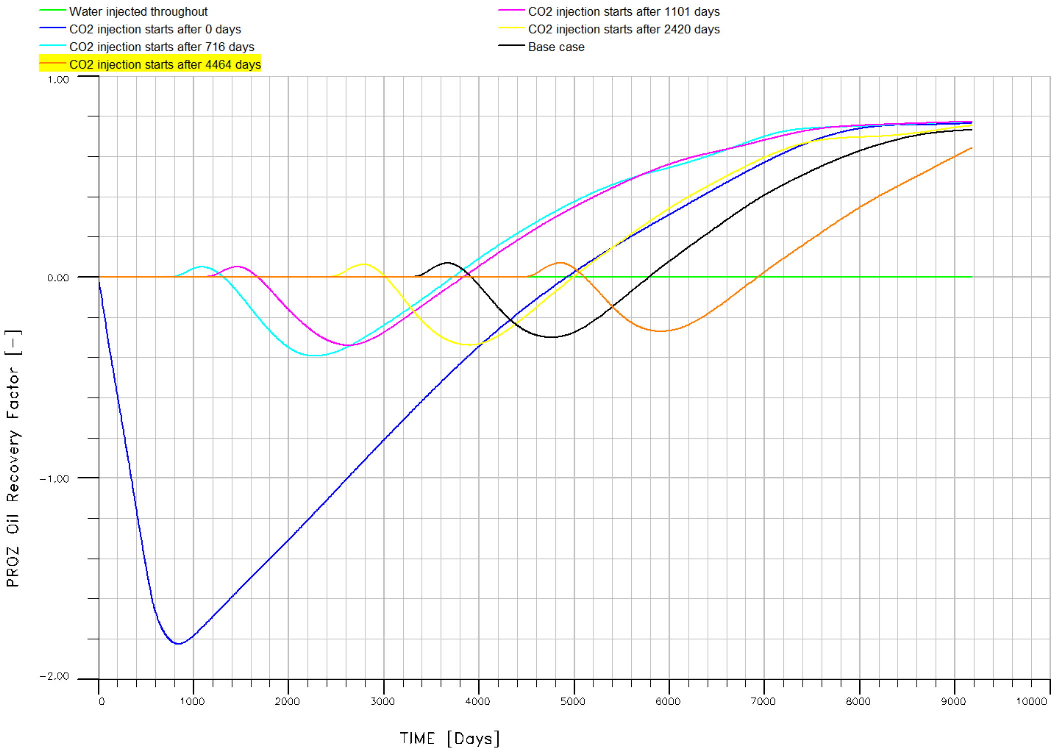

Fig. 5.8—Effect of of CO_2 injection start time on PROZ oil recovery factor. PROZ oil recovery factor is plotted versus time, for different CO_2 injection start times. The seven scenarios plotted are the; base case (black), water injected throughout(green), CO_2 injection start after 0 days (blue), CO_2 injection start after 716 days (turquoise), CO_2 injection start after 1101 days (purple), CO_2 injection start after 2420 days (yellow), CO_2 injection start after 4464 days (orange) (*figure from Office in the Schlumberger simulation launcher*).

5.3 Effect of TLMIXPAR

Fig. 5.9, **Fig. 5.10**, **Fig. 5.11** and **Fig. 5.12** show the impact of Todd-Longstaff mixing parameter, keyword TLMIXPAR in Eclipse, on the oil production rate of the field, cumulative oil production of the field, recovery factor of the MPZ, and recovery factor of the PROZ respectively. In each plot, eight different graphs are included. One graph for the case of water being injected throughout the simulation. One graph for the base case, where all parameters are as in table. 4.2. Six graphs where all parameters were being kept constant at base case values, except the Todd-Longstaff mixing parameter, which was different in all the six cases. Generally, it can be observed that the oil production increases with increasing Todd-Longstaff mixing parameter.

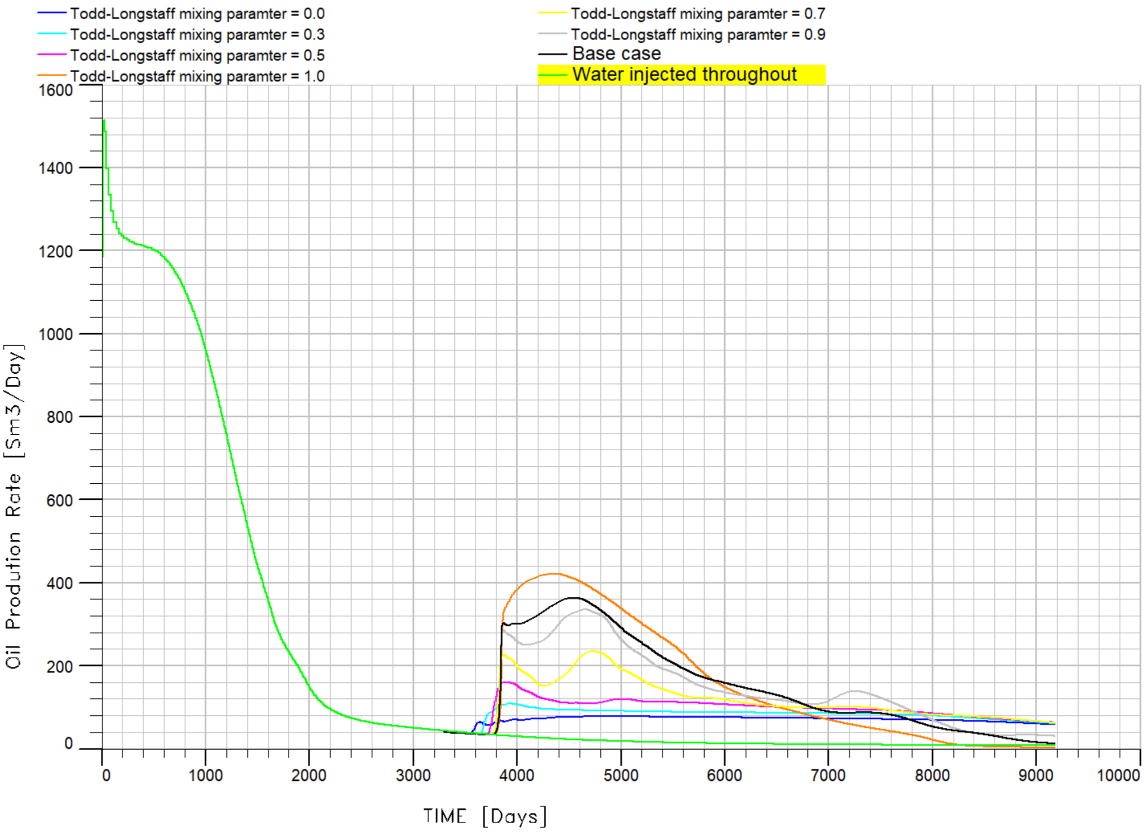

Fig. 5.9—Effect of Todd-Longstaff mixing parameter (TLMIXPAR) on oil production rate. Oil production rate is plotted versus time, for different TLMIXPAR values. The eight scenarios plotted are the; base case (black), water injected throughout(green), TLMIXPAR = 0.0 (blue), TLMIXPAR = 0.30 (turquoise), TLMIXPAR = 0.50 (purple), TLMIXPAR = 0.70 (yellow), TLMIXPAR = 0.90 (gray) and TLMIXPAR = 1.0 (orange) (*figure from Office in the Schlumberger simulation launcher*).

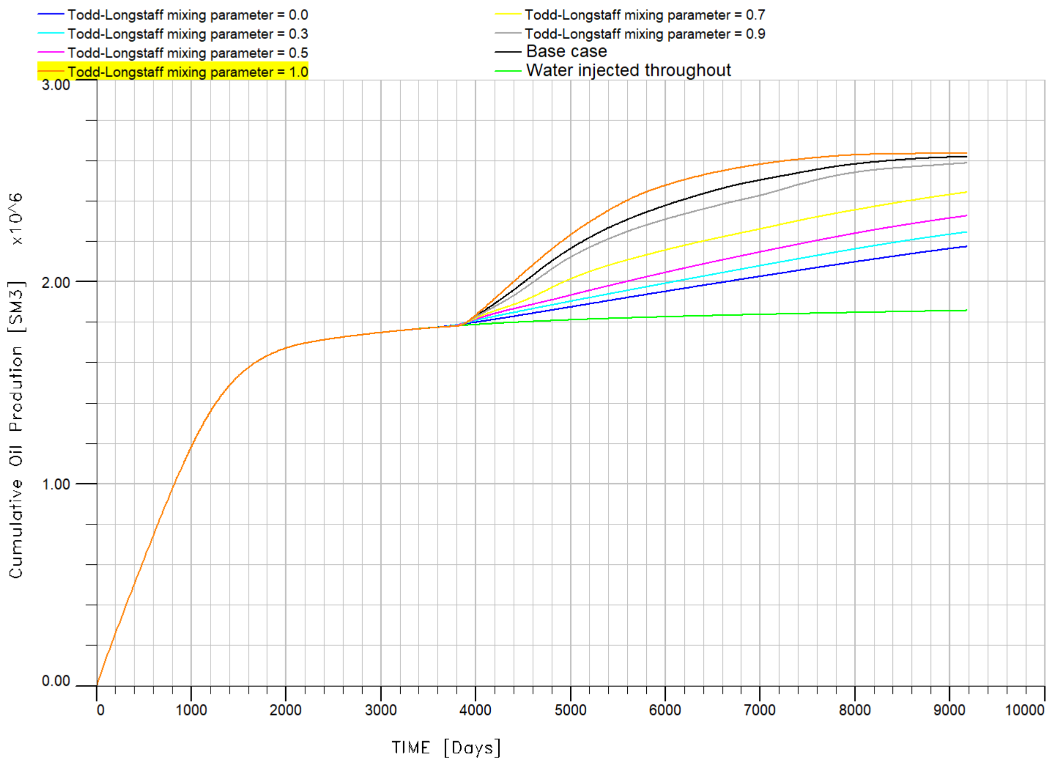

Fig. 5.10—Effect of Todd-Longstaff mixing parameter (TLMIXPAR) on cumulative oil production. Cumulative oil production is plotted versus time, for different TLMIXPAR values. The eight scenarios plotted are the; base case (black), water injected throughout(green), TLMIXPAR = 0.0 (blue), TLMIXPAR = 0.30 (turquoise), TLMIXPAR = 0.50 (purple), TLMIXPAR = 0.70 (yellow), TLMIXPAR = 0.90 (gray) and TLMIXPAR = 1.0 (orange) (*figure from Office in the Schlumberger simulation launcher*).

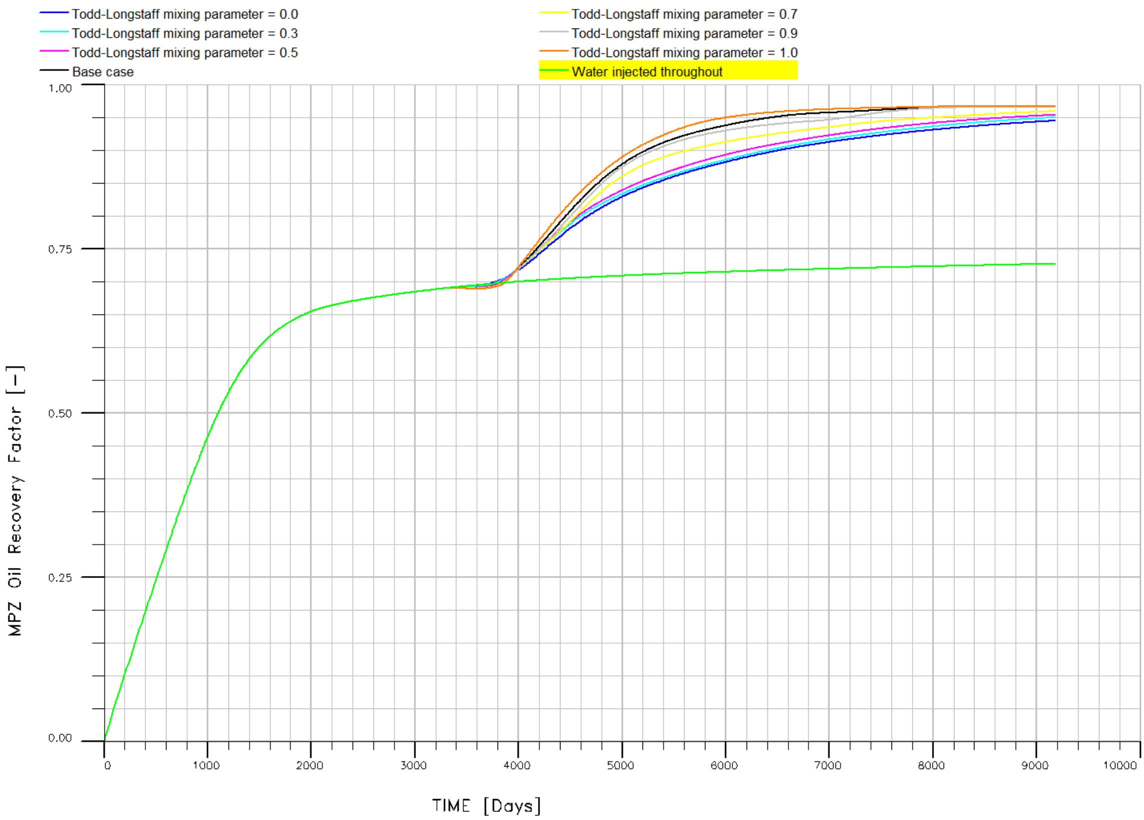

Fig. 5.11—Effect of Todd-Longstaff mixing parameter (TLMIXPAR) on MPZ oil recovery factor. MPZ oil recovery factor is plotted versus time, for different TLMIXPAR values. The eight scenarios plotted are the; base case (black), water injected throughout(green), TLMIXPAR = 0.0 (blue), TLMIXPAR = 0.30 (turquoise), TLMIXPAR = 0.50 (purple), TLMIXPAR = 0.70 (yellow), TLMIXPAR = 0.90 (gray) and TLMIXPAR = 1.0 (orange) (*figure from Office in the Schlumberger simulation launcher*).

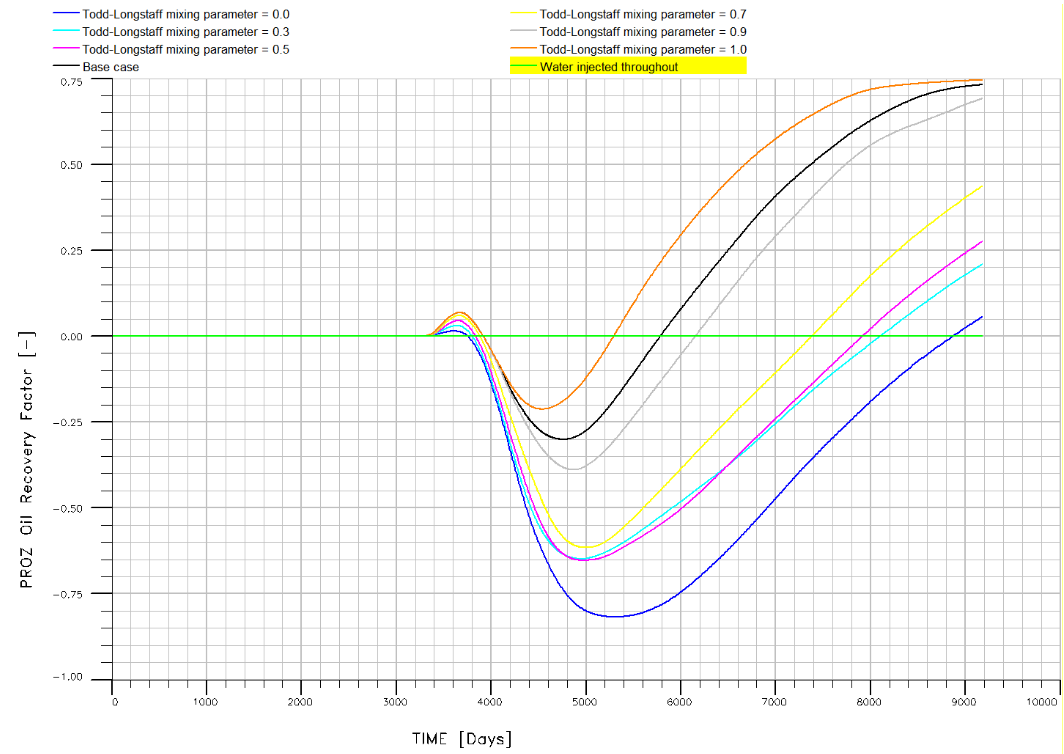

Fig. 5.12—Effect of Todd-Longstaff Mixing Parameter (TLMIXPAR) on PROZ oil recovery factor. PROZ oil recovery factor is plotted versus time, for different TLMIXPAR values. The eight scenarios plotted are the; base case (black), water injected throughout(green), TLMIXPAR = 0.0 (blue), TLMIXPAR = 0.30 (turquoise), TLMIXPAR = 0.50 (purple), TLMIXPAR = 0.70 (yellow), TLMIXPAR = 0.90 (gray) and TLMIXPAR = 1.0 (orange) (*figure from Office in the Schlumberger simulation launcher*).

5.4 Effect of SORWMIS

Fig. 5.13, **Fig. 5.14**, **Fig. 5.15** and **Fig. 5.16** show the impact of miscible residual oil saturation (the residual oil saturation after CO_2 has been injected), keyword SORWMIS in Eclipse, on the oil production rate of the field, cumulative oil production of the field, recovery factor of the MPZ, and recovery factor of the PROZ respectively. In each plot, six different graphs are included. One graph for the case of water being injected throughout the simulation. One graph for the base case, where all parameters are as in table. 4.2. Four graphs where all parameters were being kept constant at base case values, except the miscible residual oil saturation, which was different in all the four cases. Generally, it can be observed that the oil production increases with decreasing miscible residual oil saturation.

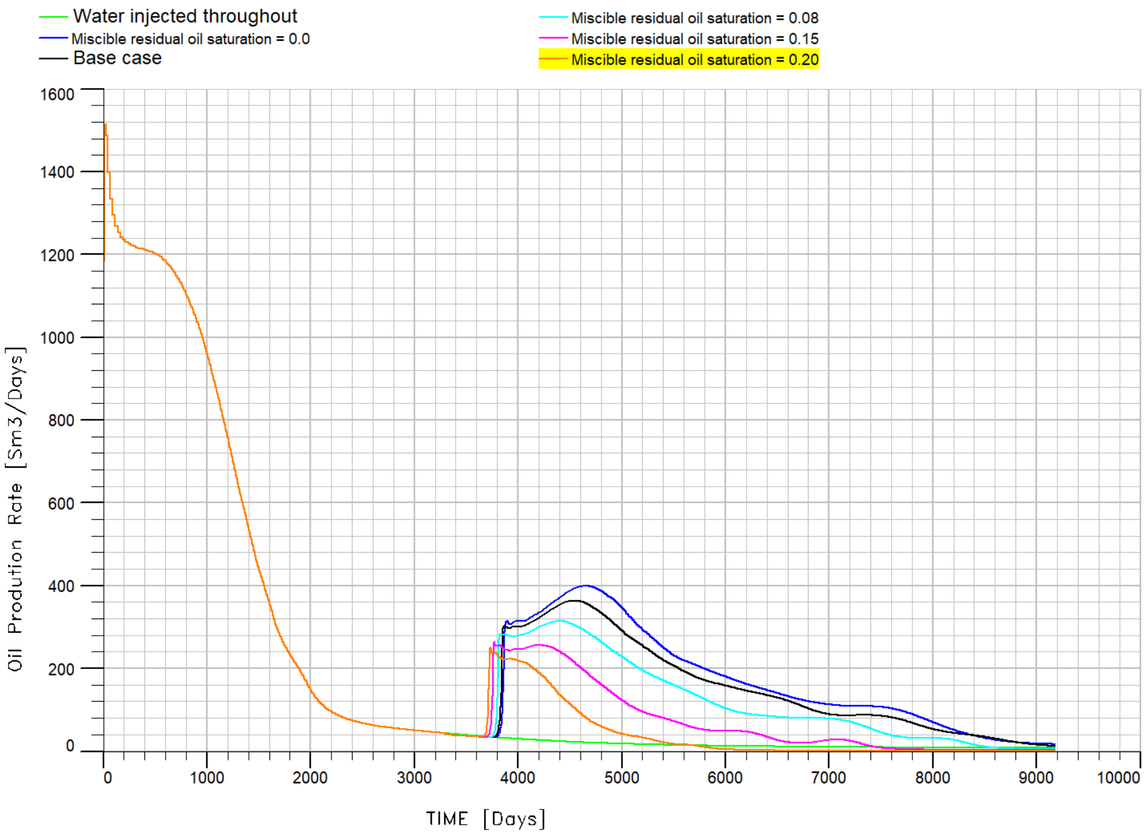

Fig. 5.13—Effect of miscible residual oil saturation (SORWMIS) on oil production rate. Oil production rate is plotted versus time, for different SORWMIS values. The six scenarios plotted are the; base case (black), water injected throughout(green), SORWMIS = 0.0 (blue), SORWMIS = 0.08 (turquoise), SORWMIS = 0.15 (purple), SORWMIS = 0.20 (orange) (*figure from Office in the Schlumberger simulation launcher*).

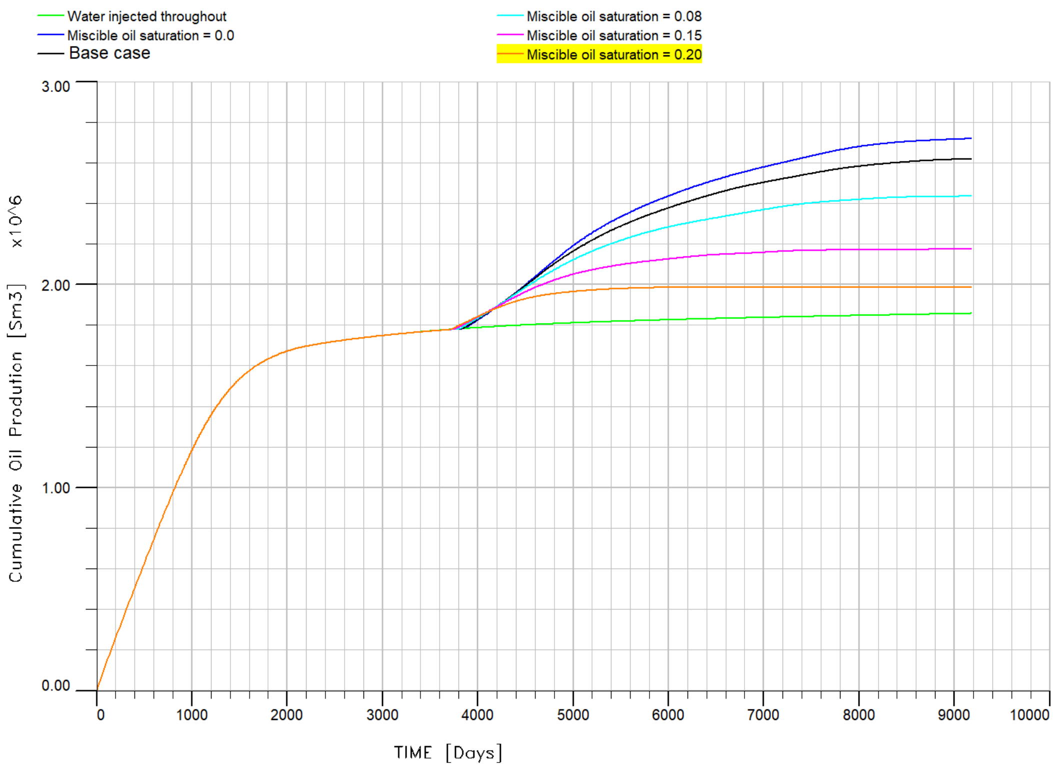

Fig. 5.14—Effect of miscible residual oil saturation (SORWMIS) on cumulative oil production. Cumulative oil production is plotted versus time, for different SORWMIS values. The six scenarios plotted are the; base case (black), water injected throughout(green), SORWMIS = 0.0 (blue), SORWMIS = 0.08 (turquoise), SORWMIS = 0.15 (purple), SORWMIS = 0.20 (orange) (*figure from Office in the Schlumberger simulation launcher*).

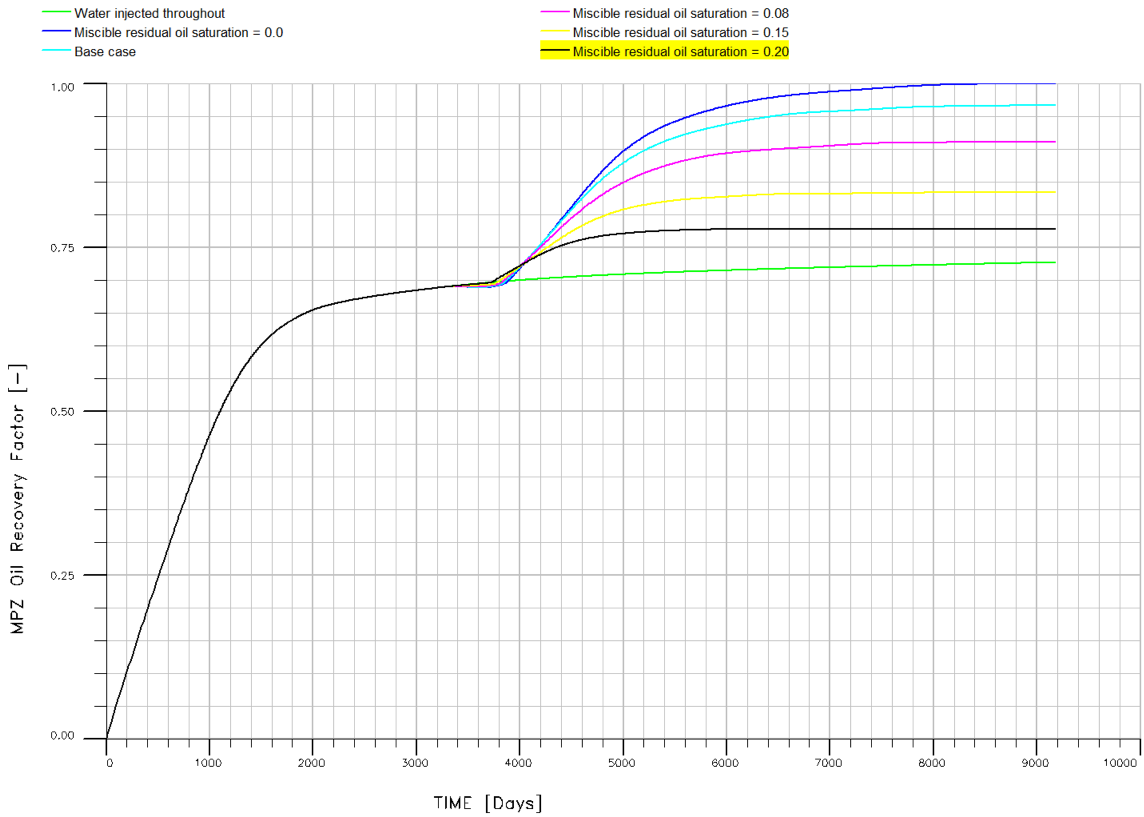

Fig. 5.15—Effect of miscible residual oil saturation (SORWMIS) on MPZ oil recovery factor. MPZ oil recovery factor is plotted versus time, for different SORWMIS values. The six scenarios plotted are the; base case (turquoise), water injected throughout(green), SORWMIS = 0.0 (blue), SORWMIS = 0.08 (purple), SORWMIS = 0.15 (yellow), SORWMIS = 0.20 (black) (*figure from Office in the Schlumberger simulation launcher*).

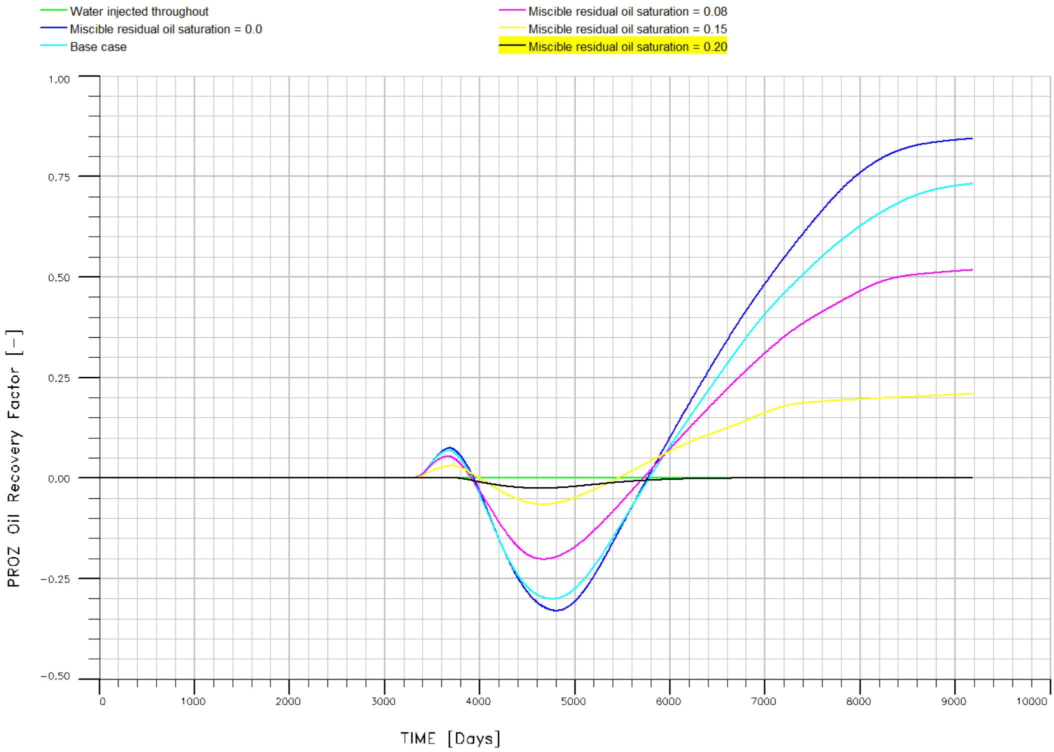

Fig. 5.16—Effect of miscible residual oil saturation (SORWMIS) on PROZ oil recovery factor. PROZ oil recovery factor is plotted versus time, for different SORWMIS values. The six scenarios plotted are the; base case (turquoise), water injected throughout(green), SORWMIS = 0.0 (blue), SORWMIS = 0.08 (purplr), SORWMIS = 0.15 (yellow), SORWMIS = 0.20 (black) (*figure from Office in the Schlumberger simulation launcher*).

Chapter 6

Discussion

In this chapter, the results presented in chapter 5 are discussed.

6.1 Effect of CO_2 Injection Rate

In all cases discussed in this section, except the one where water was injected throughout, CO_2 injection did not start until 3296 days (9.0 years) of production had passed. 1.75E+06 Sm^3 of oil, which is equivalent to a total recovery factor of approximately 0.63 had already been produced by waterflooding at that point. All this oil had been produced from the MPZ. At this point, the oil production rate was low, and CO_2 injection was commenced. Fig. 5.2 implies that the CO_2 injection rate had an enormous impact on the cumulative oil production. Increasing the CO_2 injection rate lead to significant amounts of extra oil being produced, up to a certain point. In the base case, CO_2 injection rate was equal to 1 500 000 Sm^3/d. Fig. 5.2 shows that the cumulative oil production suddenly started increasing rapidly with time, approximately 500 days (1.4 years) after CO_2 injection start, for the base case. The rapid increase indicates CO_2 breakthrough. CO_2 injection was conducted for 5880 days (16.1 years) and in the end, the cumulative oil production had increased to 2.62E+06 Sm^3, which was equivalent to a recovery factor of 0.94. That was a significant increase from the final cumulative oil production, when water injection was continued till the end. In that scenario 1.82E+06 Sm^3, equivalent to a recovery factor of 0.67, were produced. Furthermore, Fig. 5.3 and 5.4 show that no oil was produced from the paleo residual oil zone by water injection. Those figures also show that large amounts of extra oil were produced from the MPZ by CO_2 injection and that significant amounts of oil could be produced from the PROZ by CO_2 injection. Initially, the oil saturation was equal to residual oil saturation after waterflooding (S_{orw}) in the PROZ, but 73 % of that oil was produced due to CO_2 injection in the base case.

Fig. 5.2 shows that the cumulative oil production was reduced drastically as the CO_2 injection rate was reduced from the base case. With a CO_2 injection rate equal to 50 % of the base case, cumulative oil production was equal to 2.27E+06 Sm^3, which is equivalent to a recovery factor of 0.82. That was an increase of 15 percentage points from the scenario where water was injected throughout. Still, it was a decrease of 12 percentage points from the base case. Fig. 5.2 also shows that cumulative oil production started changing drastically after approximately 800 days (2.2 years). That means that the gas breakthrough was delayed with 300 days (0.8 years) compared to the base case. Fig. 5.1 shows that the oil production rate was larger after gas breakthrough in the base case than in the case with half the injection rate, until a certain point. It can also be observed that the oil production rate was getting close to zero at the end of the production for the base case, while the case with 50 % CO_2 injection rate still was producing steadily at 80 Sm^3/d. Fig. 5.4, shows that the PROZ recovery factor was negative in the end, indicating that more oil was present in the PROZ than initially was in place.

Similar trends were observed as the CO_2 injection rate varied. With lower CO_2 injection rates, the final cumulative oil production decreased, so did the oil production rate after gas breakthrough. CO_2 breakthrough was also delayed as the CO_2 injection rate was decreased. In the case of CO_2 injection rate being equal to 10 % of the base case, the cumulative oil production was lower than when water was injected throughout. As the CO_2 injection rate was increased with 25 % and 100 % from the base case, earlier CO_2 breakthrough was observed, as well as higher oil production rate the first period after breakthrough. However, the final cumulative oil production was not increased much compared to the base case. Approximately the same amount of oil was produced from the MPZ, while the PROZ recovery was somewhat increased.

Earlier CO_2 breakthrough with increasing injection rate was as expected. With higher rates the CO_2 velocity will increase and time spent on flowing from the injector to the producer will decrease. Hence, the breakthrough will occur sooner. When the CO_2 breaks through, the oil production rate increased rapidly. This is because the oil that has been contacted by the CO_2, mixes with the CO_2 and creates a new phase containing oil and CO_2, since miscible conditions were assumed, i.e. the pressure was higher than minimum miscibility pressure (MMP). Thus, amounts of oil come along with the CO_2 when it breaks through. That also explains why higher injection rates gave higher oil production rates for a period after the breakthrough. Larger amounts of the oil is contacted by CO_2 with higher CO_2 injection rates. With high injection rates, the CO_2 is pushed harder into the reservoir and manages to flow farther into the reservoir, before it rises to the top. Hence, it manages to contact and mix with more oil and therefore more oil is produced at breakthrough. Furthermore, higher CO_2 rates means that more CO_2, which is mixed with oil, manages to reach the production well in shorter time, i.e. the CO_2 production rate increases and oil rate increases as well, since oil is produced with the CO_2 as they are mixed.

Final cumulative oil production increased with increasing injection rates, up to a certain point. Several aspects contribute to that behavior. Higher rates mean that the CO_2 gets farther into the reservoir before it rises to the top. Thus, more oil is contacted by the CO_2 directly and transported to the production well. The amount of oil produced directly after being contacted by the CO_2 is higher with increasing CO_2 rates. This is a rapid process and the oil produced by this process, is produced relatively early after CO_2 breakthrough. In the case of CO_2 injection two times as large as in the base case, CO_2 is injected hard and far into the reservoir, causing most of the oil to be contacted directly by injected CO_2 and transported to the production well. That explains why most of the oil production resulting from CO_2 injection, happens at breakthrough and during a short time frame afterwards, for the case of CO_2 injection rate equal to 200 % of the base case. The second way oil is produced during CO_2 injection, is when it is not contacted directly by the injected CO_2. In that process, CO_2 have travelled a certain distance before rising to the top. Then it keeps flowing to the production well along the upper part of the reservoir. After all upper blocks has been saturated with gas and injection and production continues, the gas column will grow in z-direction. During that process oil is pushed downwards and some of the oil is forced towards the production well. This is a slow process and oil produced by this mechanism is accordingly produced at a low oil production rates. With increasing injection rates, the amount of oil produced by the first process increases, oil contacted directly by injected CO_2. The thickness of the reservoir that is produced by the first process typically increases towards the injection well. The reason for this is that close to the injection well, the CO_2 has not yet risen to the top, so even oil in the lower part of the reservoir has been contacted, if the injection well is perforated through the whole thickness. Further away from the injection well, the CO_2 starts to rise and the deeper part of the reservoir remains uncontacted by CO_2. How far the CO_2 goes before rising, is again depending on injection rate. Hence, in large parts of the reservoir, no oil from the PROZ was produced by the first process.

Based on the previous discussion, the uncommon behavior illustrated by Fig. 5.4, can be understood. The case with injection rate equal to 50 % of the base case is taken as basis. In that case, PROZ recovery factor (RF) of 0.06 was observed early after CO_2 was injected. This is a result of process one. As CO_2 is injected, oil in the PROZ near the injection well is contacted and mixed with CO_2, before being brought up with the CO_2 to the MPZ and transported to the production well. Thus, the RF goes up immediately after CO_2 injection start, since the oil recovery factor in the PROZ depends on oil volume change within the PROZ, i.e. oil transported from the PROZ to the MPZ is defined as oil produced from the PROZ. Next, the PROZ recovery factor decreased and reached a value of - 0.34. During this RF decrease period, oil is forced from the MPZ to the PROZ, as process 2 has commenced. Meaning that the gas column has started to expand in z-direction to force oil down from the MPZ to the PROZ, in areas too far away from the injector to have PROZ oil produced by direct contact with injected CO_2. Then, the RF in the PROZ started increasing again, at that time the amount of oil being produced from the PROZ to the production well due to process number 2 was higher than the amount of oil being transported from the MPZ to the PROZ as a result of process 2. In the end, the PROZ RF still is negative for the case with half the injection rate of the base, but that is misleading. Significant amounts of oil was produced from the zone, especially close to the injector. In addition, the RF was on the way up (ref Fig. 5.4), but much of the oil being produced at that time, initially belonged to the MPZ.

The final cumulative oil production increased with increasing CO_2 injection rate, partly because more oil is produced by process 1, which is a quick process. Furthermore, process 2 (CO_2 column thickness expanding in z-direction from the top) is commenced sooner and is faster with higher injection rates, despite being slow compared to process 1 (oil being contacted directly by injected CO_2). However, final cumulative oil production, did not increase substantially, when increasing the CO_2 injection rate from the base case, since most of the mobile oil was produced in the base case. Nevertheless, oil was produced sooner when increasing the injection rate.

To summarize, the simulations indicate that increasing the CO_2 injection rate will increase the cumulative oil production. However, increasing the injection rate beyond the base case value did not give significantly higher cumulative production. If the simulations were for a real field it might be of interest to increase the injection rate, because daily costs are related to production, in addition to money earned now being more worth than money earned later. Doubling the injection rate would lead to the same cumulative oil production as the base case, but after approximately 6 years of CO_2 injection instead of 16 years. Hence, the present value of the project might be higher, because the money is earned sooner and less CO_2 is injected (twice the rate for less than half the time). To do an accurate economic analysis, CO_2 prices, incentives for CO_2 sequestration, GOR, and facility costs would need to be considered. When doubling the injection rate, more advanced and expensive facilities might be needed. Also, the GOR is higher with higher rates, causing extra problems.

The validity of the simulations may also be discussed. The vast amount of oil flowing from the MPZ to the PROZ, might be unrealistic in a reservoir model more strictly based on field data, since an impermeable layer may exist between the two zones. In addition, it might be harder to make the PROZ oil flow than the MPZ oil when they are at similar saturations, because the PROZ oil properties may have been altered during the natural waterflooding that happened when the zone was formed, as stated by A. Aleidan et al. (2017).

6.2 Effect of CO_2 injection start

In the base case, the CO_2 injection started after 3296 days (9.0 years). At that time, the oil production rate due to waterflooding was low. Then, the oil production was carried out with CO_2 injection for 5880 days more, leading to a total production time of 9176 days (25.1 years). The total production time was not changed as CO_2 injection start was varied. CO_2 injection could have been conducted from the beginning, but it is often preceded by water injection until an uneconomic oil production rate is reached. Hence, that was done in this study too, for the base case. The sensitivity case where CO_2 injection started after 0 days, investigated the scenario of CO_2 being injected from the beginning. As the CO_2 injection start time was varied, all other parameters were kept constant equal to their value in the base case.

The CO_2 injection start time affects the oil production, because production behavior under CO_2 injection differs from production under the preceding water injection. This is despite the CO_2 injection rate and water injection rate being equivalent in reservoir volume. Based on Fig. 5.6, injection of CO_2 from the start (i.e. no preceding water injection) seems disadvantageous. In that scenario, the period with high production rate under waterflooding was lost. Since waterflooding normally is cheaper than CO_2 flooding, it might be disadvantageous to start injecting CO_2, when high production rates still may be achieved with water injection. Furthermore, Fig. 5.6 shows that the final cumulative oil production was lower when CO_2 was injected from the start, than what it was for the base case, despite CO_2 being injected for a longer time. That is because significant amounts of oil from the overlying zones are forced down to the water zone early on, as the injected CO_2 column starts expanding in z-direction early and forcing oil down. Substantial amounts of that oil was not produced in the end.

The case with CO_2 injection start after 716 days showed disadvantageous tendencies as well. After 716 days, the oil production rate by waterflooding was still high, approximately 1040 Sm^3/d (see Fig. 5.5). That is a high oil production rate, and it may be unnecessary costly, to start injecting CO_2, when high production rates still may be achieved by waterflooding. When CO_2 injection start was set to 1101 days, a more beneficial behavior was observed. The CO_2 injection start was delayed with approximately one year, reducing costs. Final cumulative oil production was the same as when it was injected after 716 days. The cumulative oil production almost catches up with the case of injection start after 716 days, when a total time of 4400 days has passed. At that time, the production rate was equal to 120 Sm^3/d, which may be economically beneficial, depending on costs and oil prices. Hence, injection start after 1101 days seemed more beneficial than injection start after 716 days or 0 days.

Comparing the case with injection start after 1101 days to the case with injection start after 2420 days is more complex however. The latter scenario started injecting CO_2 just after the oil production rate during waterflooding had stopped declining rapidly. At that time the oil production rate was approximately 80 Sm^3/d. Thus, the most productive potential of waterflooding had been exploited when CO_2 injection was commenced. Fig. 5.6 and 5.8 show that the final cumulative oil production was about the same, when CO_2 was injected after 2420 days, as when it was injected after 1101 days, and that recovery from the PROZ was similar. Nonetheless, CO_2 was injected for 1319 more days in the first scenario, with the same rate. Consequently, CO_2 injection costs are higher in the first case. On the other hand, oil was produced sooner in the first case and could be stopped earlier, when the process becomes uneconomical. In addition, more oil was produced sooner, which means that money is generated earlier, and a fixed amount of money is worth more the sooner it is earned (the present value is higher). Also, the water injection costs are lower in the first case.

The two cases where CO_2 was injected later than 2420 days showed similar trends as when it was injected after 2420 days. The main difference was that oil was produced later and with the latest injection start, the final cumulative production was lower.

The simulations give an idea of when it is most beneficial to start the CO_2 injection, depending on oil production development under waterflooding. A general trend is that it is beneficial to start the CO_2 injection immediately after the oil production rate has stopped declining rapidly under waterflooding, and reached a low production rate, if water injection potential is supposed to be exploited. On the other hand, it was observed that it could be beneficial to start injecting CO_2 while the oil production rate under waterflooding was declining, but still was high. It was also noticed that CO_2 injection from the beginning was unbeneficial, if oil may be produced effectively by water injection. However, when planning the development of a field, other aspects must be taken into account. It might be expensive to change a well from a water injector to a CO_2 injector and it takes time which delays revenue. The infrastructure might need to account for water injection, if it was not planned otherwise. These are arguments that support CO_2 injection from the beginning. Availability of CO_2 is also important and puts a restriction on how long CO_2 can be injected with a given rate. That may be an argument for delaying the injection until oil cannot be produced economically by waterflooding. When the CO_2 EOR facilities can be ready to use is also of importance, when deciding CO_2 injection start.

6.3 Effect of Todd-Longstaff Mixing Parameter

The Todd-Longstaff mixing parameter is a central parameter in the Eclipse 100 (black oil) miscible flood modeling. It is an empirical parameter and controls the degree of mixing within each grid block. The keyword for the parameter in Eclipse is TLMIXPAR. Fig. 5.9 to Fig. 5.12 illustrate the effect of Todd-Longstaff mixing parameter, ω. Fig. 5.9 shows production rate versus time. In the graphs, CO_2 breakthrough can be recognized as the point where the oil production rate suddenly increases abruptly after a period of low production rate. The time of breakthrough was delayed with increasing value of ω. With ω equal to 1, breakthrough occurred 200 days later than with ω equal to 0. Furthermore, the production rate was higher at breakthrough and for some period after, with larger ω. The reason for this is that the first CO_2 that breaks through is a hydrocarbon phase that is a mix of oil and CO_2. With large ω, the degree of mixing is large. Hence, the injected CO_2 that mixes with oil under miscible conditions, gets a larger proportion of oil and therefore more “oil-like” attributes. Consequently, the mix moves somewhat slower, but a larger fraction of the mix is oil, causing the breakthrough to happen later, but with a higher fraction of oil which cause higher oil production rate. More precisely, beneficial mobility ratio was achieved with large ω, causing a better sweep efficiency. Smaller ω may be a way of capturing fingering effects.

Fig. 5.11 and 5.12 illustrate that it was especially the PROZ that was affected by ω. That may be explained by the fact that ω controls degree of mixing. Lower degree of mixing with the heavier oil means that the CO_2 starts rising sooner and a smaller part of the shallower zones, including PROZ, is contacted directly by CO_2.

For simulations on reservoir models solely based on data from a specific field, deciding a reasonable value of ω is complex. The parameter affects oil production behavior and consequently predicted present value of the project. However, it is an empirical parameter and it is usually intricate to conclusively decide it based on physical properties of the reservoir and fluids. Nonetheless, the value of ω says something about the mixing of CO_2 and oil, and information about CO_2 purity, oil composition, pressure, and temperature can give an indication of how to the value should be defined, but that is unlikely. It is more common to vary the parameter based on heterogeneities in the reservoir. For practical purposes, the parameter is often used as a history matching parameter.

The Todd-Longstaff mixing parameter is an empirical parameter with high uncertainties related to it. Therefore, modeling miscible CO_2 EOR with the Todd-Longstaff parameter has weaknesses, compared to doing it with a compositional model. In a compositional model, the mixing is based on physical properties to a larger degree. In addition, compositional models get across component transfer between oil components and CO_2 more easily. Yet, the Todd-Longstaff model is less computational heavy, takes shorter time and may give plausible estimates. Companies may for instance use it as a preliminary study of CO_2 EOR.

6.4 Effect of Miscible Residual Oil Saturation

The miscible residual oil saturation is the residual oil saturation after CO_2 and oil has mixed. The Eclipse keyword for the parameter is SORWMIS, which it hereby will be referred to as. Fig. 5.14, shows that the cumulative oil production was increased when lower SORWMIS values were used. That is because every part of the reservoir may be drained down to a lower oil saturation, when the residual oil saturation decreases. Fig. 5.13 shows that breakthrough of CO_2 happened later when SORWMIS had smaller values. This is because lower residual oil saturation means that more oil can be mixed and carried by the CO_2, making propagation of the CO_2 front moderately slower. However, the oil production rate was higher a period after CO_2 breakthrough with lower residual oil saturation, since more oil was produced together with the CO_2.

Fig. 5.15 and 5.16 show that both PROZ and MPZ were significantly influenced by SORWMIS. The residual oil saturation before CO_2 injection was equal to 0.20. When the residual oil saturation was decreased, more oil was produced from both zones. To produce anything from the PROZ, the residual oil saturation had to be decreased, because the initial oil saturation throughout that zone was equal to the residual oil saturation. In the MPZ, oil recovery was increased compared to the case with water injected throughout. That was because effects of miscible CO_2 injection were seen in parts of the reservoir where the oil saturation was higher than residual oil saturation. Nevertheless, amounts of oil produced increased in both zones, with decreasing residual oil saturation.

Unlike the Todd-Longstaff mixing parameter, the residual oil saturation after CO_2 injection is a physical parameter. Laboratory tests may be conducted to help decide a reasonable value for the parameter. Yet, it can be hard to predict. Heterogeneities in the reservoir may lead to unforeseen different values in different parts of the reservoir. For example, due to wettability variations. The synthetic box model used in this thesis was assumed to be homogenous and did not capture these variations. These variations can be tough to capture in real models too, since laboratory tests only would be run on a few cores that might not be in native or restored state.

To physically alter the residual oil saturation after miscible CO_2 injection in a system would not be the objective. When CO_2 with a fixed purity is injected, a given system will get a new residual oil saturation which depends on reservoir conditions and reservoir shape and properties. This miscible residual oil saturation may vary in the reservoir. The objective would be to evaluate how oil production is affected by the parameter, since uncertainties are related to it.

6.5 Joint Discussion

The focus in section 6.1 – 6.4 was on the effect different parameters had on oil production. For commercial purposes however, companies have to take into account the gas-oil-ratio (GOR) and water cut, since expenditures come along with high water cut and GOR. For all sensitivity analysis conducted, the water cut was high before injection of CO_2 started. This could be due to water coning. The production well was only perforated in the MPZ, but since the deepest perforation was 5 m above the PROZ, water coning may have happened. When injected CO_2 broke through, the water production rate quickly dropped.

The GOR was low before the CO_2 was injected. The minimum bottomhole pressure was 77 bar higher than the bubble point pressure. Hence, the pressure in the reservoir was above the bubble point pressure at any time. Consequently, there was no free gas in the reservoir when water was injected. Therefore, the GOR was equal to the solution gas-oil ratio before CO_2 injection started. When CO_2 breaks through, the GOR increased in all cases, but remained on manageable levels in all cases until a certain point, where it reached too high values to be economically justifiable. The general trend was that GOR increased to high values sooner in the cases where oil was produced earlier. That is sensible since GOR is volume of gas produced divided by volume of oil produced. When oil is produced sooner, the oil production rate drops earlier and the denominator in GOR becomes smaller, leading to a higher value of GOR.

Costs are related to separation of oil from water and from gas and when the GOR or water cut is above a certain value, the oil production and processing will be too expensive relative to the revenue from selling the oil. Some of the produced CO_2 may be separated and re-injected, thus saving costs related to buying new CO_2. However, the reinjected CO_2 must go through costly processes like separation and compression.

6.6 Recommendations for Further Work

Limitations of the simulations conducted on the syntheic model has been pointed out. In this section recommendations for further work is presented.

- Similar simulations to what have been executed in this thesis should be performed on a reservoir model of a real field, with an associated paleo residual oil zone.

- For the field to be investigated, fluid analysis of the paleo oil should be conducted, and properties of the paleo oil should be compared to the MPZ oil, down to molecular level

- A compositional model should be acquired. Next, simulations with a compositional model should be compared to simulations with a black oil model.

- In addition to controlling the oil production with a maximum oil production rate and minimum bottomhole pressure, a maximum GOR and water cut can be introduced, based on information about water and gas handling costs.
- Economic evaluation of oil production projects can be performed for the different sensitivity analysis. Information about taxes, CO_2 costs, separation and compression costs, facility costs, and other costs should be obtained to do such an analysis.

Chapter 7

Conclusion

Literature studies about paleo residual oil zones and CO_2 EOR were conducted. Furthermore, simulations were conducted on a synthetic reservoir model with a paleo residual oil zone, to qualitatively assess effect of various parameters in CO_2 EOR projects. The main findings of the literature studies and simulations were as follows:

- Restricted amounts of literature has been published about paleo residual oil zones, since these zones were assumed to be unproducible before modern EOR methods.
- Three mechanisms causing PROZs have been explained, and since one of these often has occurred at some point in time, the spread of PROZs is substantial.
- Previous CO_2 EOR projects in fields with a PROZ have given promising results, despite public literature about such studies being restricted.
- Core analysis performed by A. Aleidan et al. (2017) illustrated that paleo oil may have significantly different properties than the MPZ oil, when inspecting on a molecular level. This could be the case even if the two oils have the same source rock and apparently have similar properties based on primary inspection.
- In the past, CO_2 injection has proved effective considering the price, compared to injection of other gases or similarly miscible fluids.
- Oil production was sensitive to changes of all four parameters investigated in the sensitivity analysis.

- General trends were that more oil was produced sooner with increased CO_2 injection rate. Earlier CO_2 injection start caused more oil to be produced sooner, except when it was injected from day 0. However, it seemed more beneficial to start injecting CO_2 immediately after oil production had stabilized at a low production rate under waterflooding.

- A shortcoming of the sensitivity analysis was that quantitative net present value (NPV) assessment of the different cases were not performed, due to lack of accurate cost data related to CO_2 EOR projects. However, economics discussion was included in the discussion.

- Uncertainties were related to the validity of the simulations, as the model assumed similar paleo and MPZ oil, a black oil model was used, the reservoir model was synthetic, and assumed homogeneity.

- Due to the simplicity of the model, some mechanisms were lost. However, a strength of the simplicity was that effect of parameter variations could be interpreted easily. In addition, measures were done to make the model realistic enough.

- Higher values of Todd-Longstaff mixing parameter and lower values of SORWMIS seemed beneficial, but these are not easily controlled in practice.

- Due to the high costs related to CO_2 EOR projects, it seems unlikely to be beneficial to commence CO_2 EOR in the PROZ unless the MPZ can benefit from CO_2 EOR. In the simulations in this thesis, most of the extra oil from CO_2 EOR was produced from the MPZ.

- Tax incentives due to CO_2 sequestration, or already existing nearby CO_2 injection infrastructure, may lower the threshold to commence a CO_2 EOR project.

Nomenclature

B_n	=	formation volume factor of fluid n, rm^3/Sm^3
k_{rg}	=	relative permeability of gas, unitless
k_{rn}	=	relative permeability of hydrocarbon phase, unitless
k_{ro}	=	relative permeability of oil, unitless
S_g	=	saturation of gas, unitless
S_{gc}	=	critical gas saturation, unitless
S_n	=	saturation of hydrocarbon phase, unitless
S_o	=	saturation of oil, unitless
S_{or}	=	residual oil saturation, unitless
S_{orw}	=	residual oil saturation to waterflooding, unitless
S'_g	=	S_g - S_{gc}, unitless
S'_n	=	S'_o - S'_g, unitless
S'_o	=	S_o - S_{or}, unitless
$(\frac{S_o}{S_n})_{ge}$	=	effective saturation fraction for gas density calucations, unitless
$(\frac{S_o}{S_n})_{oe}$	=	effective saturation fraction for oil density calucations, unitless
$V_{n_{res}}$	=	reservoir volume of fluid n, rm^3
$V_{n_{surf}}$	=	surface volume of fluid n, Sm^3
μ_g	=	gas viscosity, cP
μ_m	=	mixture viscosity, cP
μ_o	=	oil viscosity, cP
$\mu_{n_{eff}}$	=	effective viscosity of fluid n, cP
ω	=	Todd-Longstaff mixing parameter
ρ_g	=	gas density, kg/m^3
ρ_o	=	oil density, kg/m^3
$\rho_{g_{eff}}$	=	effective gas density, kg/m^3
$\rho_{o_{eff}}$	=	effective oil density, kg/m^3

Abbreviations

API	=	American Petroleum Institute
EOR	=	Enhanced Oil Recovery
MMP	=	Minimum Miscibility Pressure
MPZ	=	Main Pay Zone
NCS	=	Norwegian Continental Shelf
NPV	=	Net Present Value
OWC	=	Oil Water Contact
PROZ	=	Paleo Residual Oil Zone
PVT	=	Pressure Volume Temperature
RF	=	Recovery Factor
SORWMIS	=	Eclipse keyword for miscible residual oil saturation
TLMIXPAR	=	Eclipse keyword for Todd-Longstaff mixing parameter

References

Aleidan, A.A., Zhou, X., Kwak, H., et al. (2014). A Laboratory Study to Investigate CO2 Potential to Mobilize Paleo Oil. Presented at the SPE Improved Oil Recovery Symposium. DOI: `10.2118/169113-ms`.

Aleidan, A., Kwak, H., Muller, H., et al. (May 2017). Residual-Oil Zone: Paleo-Oil Characterization and Fundamental Analysis. *SPE Reservoir Evaluation & Engineering* **20** (02): 260–268. DOI: `10.2118/179545-pa`.

Beeson, D. and Ortloff, G. (Apr. 1959). Laboratory Investigation of the Water-Driven Carbon Dioxide Process for Oil Recovery. *Journal of Petroleum Technology* **11** (04): 63–66. DOI: `10.2118/1100-g`.

Bergmo, P.E., Grimstad, A.-A., and Kurtev, K. (2018). *Mapping of Paleo Residual Oil Zones on the NCS and the Potential for Production by CO2-EOR.*

Bush, J. (2001). The Seminole San Andres Unit Residual Oil Zone (ROZ) CO2 Flood. Presented at the CO2 Flooding Conference, Midland, TX.

Crawford, H., Neill, G., Bucy, B., et al. (Mar. 1963). Carbon Dioxide - A Multipurpose Additive for Effective Well Stimulation. *Journal of Petroleum Technology* **15** (03): 237–242. DOI: `10.2118/571-pa`.

Harouaka, A., Trentham, B., and Melzer, S. (2013). Long Overlooked Residual Oil Zones (ROZ&aposs) Are Brought to the Limelight. Presented at the SPE Unconventional Resources Conference Canada. DOI: `10.2118/167209-ms`.

Holm, L. (Aug. 1986). Miscibility and Miscible Displacement. *Journal of Petroleum Technology* **38** (08): 817–818. DOI: `10.2118/15794-pa`.

Holm, L. and Josendal, V. (Dec. 1974). Mechanisms of Oil Displacement By Carbon Dioxide. *Journal of Petroleum Technology* **26** (12): 1427–1438. DOI: `10.2118/4736-pa`.

Holm, L. (1963). CO2 Slug and carbonated water oil recovery processes. *Producers Monthly* **27** (9): 6–8.

Jones, P.J. and Tobey, M.H. (Feb. 1999). *Pyrolytic Oil-Productivity Index Method for Characterizing Reservoir Rock*. U.S. Patent Number 5,866,814.

Koperna, G. and Kuuskraa, V. (2006a). Technical oil recovery potential from residual oil zone: Williston Basin. *US Depertment of Energy: Washington, DC, USA*.

Koperna, G. and Kuuskraa, V. (2006b). Technical Oil Recovery Potential from Residual Oil Zones: Permian Basin. *US Depertment of Energy: Washington, DC, USA*.

Koperna, G. and Kuuskraa, V. (2006c). Technical oil recovery potential from residual oil zones: Permian Basin. *US Depertment of Energy: Washington, DC, USA*.

Liu, K., Pang, X., Jiang, Z., et al. (Apr. 2006). Quantitative estimate of residual or palaeo-oil column height. *Journal of Geochemical Exploration* **89** (1-3): 239–242. DOI: `10.1016/j.gexplo.2005.11.053`.

McKean, T., Thomas, A., Chesher, J., et al. (1999). Schrader Bluff CO2 EOR Evaluation. Presented at the SPE Western Regional Meeting. DOI: `10.2118/54619-ms`.

Melzer, L.S. (2006). Stranded Oil in the Residual Oil Zone. *Report for Advanced Resources International and US Department of Energy*.

Melzer, L.S., Kuuskraa, V.A., and Koperna, G.J. (2006). The Origin and Resource Potential of Residual Oil Zones. Presented at the SPE Annual Technical Conference and Exhibition. DOI: `10.2118/102964-ms`.

Menzie, D. and Nielsen, R. (Nov. 1963). A Study of the Vaporization of Crude Oil by Carbon Dioxide Repressuring. *Journal of Petroleum Technology* **15** (11): 1247–1252. DOI: `10.2118/568-pa`.

NationalPetroleumCouncil, ed. (1976). *Enhanced oil recovery–an analysis of the potential for enhanced oil recovery from known fields in the United States–1976–2000*. Washington DC.

Pang, H., Chen, J., Pang, X., et al. (Dec. 2012). Estimation of the hydrocarbon loss through major tectonic events in the Tazhong area, Tarim Basin, west China. *Marine and Petroleum Geology* **38** (1): 195–210. DOI: `10.1016/j.marpetgeo.2011.11.006`.

PTRC (2014). *What is CO2-EOR*. URL: `https://hub.globalccsinstitute.com/publications/what-happens-when-co2-stored-underground-qa-ieaghg-weyburn-midale-co2-monitoring-and-storage-project/8-what-co2-eor` (visited on 07/03/2018).

Rosman, A. (1977). Experimental Studies Of Low Ift Displacement By CO2 Injection. Presented at the SPE Annual Fall Technical Conference and Exhibition. DOI: `10.2118/6723-ms`.

Schlumberger (2016). *Eclipse Technical Description.*

Simon, R. and Graue, D. (Jan. 1965). Generalized Correlations for Predicting Solubility, Swelling and Viscosity Behavior of CO2 -Crude Oil Systems. *Journal of Petroleum Technology* **17** (01): 102–106. DOI: 10.2118/917-pa.

Skauge, A. and Surguchev, L. (2000). Gas Injection in Paleo Oil Zones. Presented at the SPE Annual Technical Conference and Exhibition. DOI: 10.2118/62996-ms.

Stalkup, F. (Aug. 1978). Carbon Dioxide Miscible Flooding: Past, Present, And Outlook for the Future. *Journal of Petroleum Technology* **30** (08): 1102–1112. DOI: 10.2118/7042-pa.

Trentham, B., Melzer, S., and Vance, D. (2012). *Commercial exploitation and the origin of residual oil zones: Developing a case history in the Permian Basin of New Mexico and West Texas: RPSEA.*

Yang, C. (2014). *A Preliminary Investigation of Possible Occurrences of Transition Zones and Residual Oil Zones Below Oil-Water Contact in Matured Oil Fields, Southeast Saskatchewan.* MS thesis. Faculty of Graduate Studies and Research, University of Regina.

Zhang, Y., Zhang, L., Niu, A., et al. (2010). Integrated Assessment of CO2 Enhanced Oil Recovery and Storage Capacity. Presented at the Canadian Unconventional Resources and International Petroleum Conference. DOI: 10.2118/137615-ms.